UvA-DARE (Digital Academic Repository)

Distributions and habitats of the two partly allopatric cryptic species of the vulnerable moss Hamatocaulis vernicosus (Bryophyta) in Europe

Hedenas, L.; Collart, F.; Heras, P.; Infante, M.; Kooijman, A.; Kučera, J.

Distributions and habitats of the two partly allopatric cryptic species of the vulnerable moss *Hamatocaulis vernicosus* (Bryophyta) in Europe

LARS HEDENÄS[1,*,], FLAVIEN COLLART[2,], PATXI HERAS[3], MARTA INFANTE[3], ANNEMIEKE KOOIJMAN[4] and JAN KUČERA[5]

[1]*Department of Botany, Swedish Museum of Natural History, Box. 50007, SE-104 05 Stockholm, Sweden*
[2]*Department of Ecology and Evolution (DEE), University of Lausanne, Switzerland*
[3]*Museo de Ciencias Naturales de Álava, Fundadora de las Siervas de Jesús, 24. 01001 Vitoria, Spain*
[4]*Department of Ecosystem and Landscape Dynamics, Institute for Biodiversity and Ecosystem Dynamics (IBED), University of Amsterdam, P.O. Box 94240, NL-1090 GE Amsterdam, the Netherlands*
[5]*Department of Botany, Faculty of Science, University of South Bohemia, Branišovská 1760, 370 05 České Budějovice, Czech Republic*

The geographical distributions of the two cryptic species of the wetland moss *Hamatocaulis vernicosus* were mapped for western, central and northern Europe, based on identifications of the two by the nuclear ITS1 + 2 and the plastid *rpl16* and *trnL–trnF*. The distributions of the two cryptic species overlap to a large extent. However, in the west and south-west only cryptic species 1 is present, whereas in the boreal north only cryptic species 2 occurs, which agrees with its distribution in Scandinavia. Despite these differences in distribution, no differences between the two cryptic species were revealed in habitat water chemistry, elevation distribution or climatic niches. The difference in distribution therefore suggests that cryptic species 1 could have survived the glacial period in southern Europe and cryptic species 2 in northern or eastern Europe. However, the studied molecular markers did not reveal geographical patterns suggesting origins in different glacial refugia. Although populations of both cryptic species have decreased in large portions of western Europe, a significantly negative Tajima's *D* may reflect the long-term expansion south of Scandinavia since the glacial bottleneck, potentially correlated with the expansion of earlier extensive agricultural management of wetlands.

ADDITIONAL KEYWORDS: climatic niche – conservation – EU Habitat Directive – glacial refugia – water chemistry – wetland mosses.

INTRODUCTION

Cryptic species are molecularly distinct but morphologically indistinguishable. They are relatively frequent in many organism groups (Bickford *et al.*, 2006; Pérez-Ponce de León & Poulin, 2016; Poulin & Pérez-Ponce de León, 2017; Struck *et al.*, 2018), especially in bryophytes (Heinrichs *et al.*, 2009; Hedenäs, 2020a,b), in which reduced morphologies necessitate phylogenetic testing of species delimitations (Vanderpoorten & Shaw, 2010). The most thoroughly studied cryptic moss species in western and central Europe are those

of *Hamatocaulis vernicosus* (Mitt.) Hedenäs, a flagship species in mineral-rich fens that is protected by the European Habitat Directive (Anonymous, 1992). After its two cryptic species were revealed (Hedenäs & Eldenäs, 2007), they were thoroughly studied in Sweden (Hedenäs, 2018) and especially in the Czech Republic (Manukjanová *et al.*, 2019a; Manukjanová, Štechová & Kučera, 2019b), but information regarding their occurrences in other portions of the continent is more anecdotal. A comprehensive morphological evaluation revealed no morphological differences between the two (Manukjanová *et al.*, 2019a).

With the mounting evidence for cryptic speciation and for strong geographical structure of phylogenetic

*Corresponding author. E-mail lars.hedenas@nrm.se

differentiation within bryophyte species (Hedenäs, 2016, 2018, 2019), ecotype formation has also raised concerns of bryologists (Collart *et al.*, 2021). The mounting evidence for cryptic speciation and strong geographical structure within phylogenetically redefined species among bryophytes has raised concerns that ecotype differentiation may also occur. Unlike many seed plants, bryophytes supposedly do not develop ecotypes, but rather display an inherent broad ability to cope with environmental variation (see review by Patiño & Vanderpoorten, 2018). Bryophytes in general disperse across long distances, so that even distant populations may regularly reshuffle their genetic variability, possibly neutralizing local adaptations (Mikulášková *et al.*, 2015). Nevertheless, reports of regional differences in niche characteristics (Shaw, 1985; Vanderpoorten & Durwael, 1999; Graham *et al.*, 2019) and mounting evidence for correlated patterns of genetic divergence and environmental variation (Hutsemékers *et al.*, 2010; Pisa *et al.*, 2013; Mikulášková *et al.*, 2015; Magdy *et al.*, 2016), suggest that adaptation may play a more important role in bryophytes than previously thought. If ecological specialization occurs in different lineages within species or in cryptic species, this could challenge the application of species distribution models at the species level (Pearman *et al.*, 2010; Smith *et al.*, 2019; Collart *et al.*, 2021).

Hedenäs & Eldenäs (2007) and Hedenäs (2018) speculated on explanations for the European distributions of the two cryptic species of *H. vernicosus*, but this was based on a too limited sampling for a more conclusive elucidation. Hedenäs & Eldenäs (2007) found no differences in pH and electric conductivity (EC) between the habitats of the two, and Manukjanová *et al.* (2019a) found no differences in several studied climatic parameters. However, these studies were geographically limited, and a wider sampling is needed to decide whether niche differentiation could explain distribution patterns on a continental scale.

Hamatocaulis vernicosus is classified as vulnerable by the IUCN (Hodgetts *et al.*, 2019) and is included in Appendix II of the EU Habitat Directive (Anonymous, 1992) as a species for which it is mandatory for EU member states to ensure its survival. Since we now know that *H. vernicosus* includes two cryptic species that are necessarily less common than the morphology-defined species, we need more accurate information for their efficient conservation. We know that cryptic species 1 (from now on called CRS1), the southern cryptic species of Hedenäs (2018), is not found in northern Sweden, where only cryptic species 2 (CRS2; the northern cryptic species) occurs. In the Czech Republic, CRS1 occurs on 93% of the *H. vernicosus* localities, whereas CRS2 only occurs at 11%; 7% of the

sites support a mixed occurrence of the two species (Manukjanová *et al.*, 2019a). However, as we do not know how the two cryptic species are distributed in most of Europe, with what frequency and under which habitat and climatic conditions, an efficient continental conservation strategy is difficult to enforce.

In this study, we include > 200 samples of *H. vernicosus* from Europe eastwards to Finland, westernmost Russia, Estonia, Poland and Romania and a few samples from other continents. We have three main aims with this investigation: (1) to reveal the geographical distributions of CRS1 and CRS2 in the mentioned portions of Europe; (2) to quantify their European genetic diversity and the variation within and between the two cryptic species; and (3) to explore whether differences in habitat and climatic preferences in Europe can potentially explain differences in their geographical distributions. Alternatively, do intraspecific patterns of genetic variation support different post-glacial histories that may explain their different extant distributions?

MATERIAL AND METHODS

STUDIED MATERIAL

A brief characterization of *H. vernicosus* is found in Hedenäs (2018). The species is widely distributed but rarely common in the northern temperate to Arctic zones and has scattered occurrences in the mountains of central and northern South America (Hedenäs, 2003). Sweden was well represented in the earlier studies based on the molecular markers used here (Hedenäs & Eldenäs, 2007; Hedenäs, 2018), and we therefore added samples of *Hamatocaulis vernicosus s.l.* only from other portions of Europe, as delimited previously. We generated new sequences from 91 European samples and one extra-European sample in addition to the 113 European and 12 extra-European samples available from the earlier studies, yielding a total of 204 European and 13 extra-European samples. One sample of each of the species *Hamatocaulis lapponicus* (Norrl.) Hedenäs, *Scorpidium cossonii* (Schimp.) Hedenäs, *S. revolvens* (Sw. ex Anonymo) Rubers and *S. scorpioides* (Hedw.) Limpr. were included as the outgroup to explore the relationship between the two cryptic species of *H. vernicosus* in a broader context. For locality data, see Appendix 1.

MOLECULAR METHODS

We studied the same three molecular markers as in the earlier investigations (Hedenäs & Eldenäs, 2007; Hedenäs, 2018), the nuclear internal transcribed spacers 1 and 2 (ITS) and the plastid ribosomal protein

16 G2 intron (*rpl16*) and the *trnL* intron + the $trnL_{UAA}$-$trnF_{GAA}$ intergeneric spacer (*trnL–trnF*). The molecular laboratory work was performed following Hedenäs & Eldenäs (2007) and Hedenäs (2018).

SEQUENCE EDITING AND ANALYSES

We edited and assembled nucleotide sequence fragments for each DNA region using PhyDE v.0.9971 (http://www.phyde.de/index.html; accessed 2 March 2021). We aligned the assembled sequences manually in PhyDE. Regions of partially incomplete data at the beginning and end of the sequences were identified and were excluded from subsequent analyses. Gaps were coded using the simple indel coding of Simmons & Ochoterena (2000) in SeqState (Müller, 2005) and this information was included in the analyses. The sequence alignments used in the analyses are available on request. GenBank accession numbers are listed in Appendix 1.

Although ITS paralogues are occasionally encountered in bryophytes (see, e.g. Košnar *et al.*, 2012; Hedenäs, Heinrichs & Gallego, 2019), ITS chromatograms included in this study did not show 'messy' patterns or noise that could suggest paralogy, and the 5.8S gene was invariable among all samples (cf. Shaw *et al.*, 2002; Feliner & Rosselló, 2007). Therefore, the revealed ITS variation was interpreted as being among homologous ribotypes.

We tested whether two cryptic species exist among the specimens of *H. vernicosus s.l.* with all three markers available in the online assemble species by automatic partitioning (ASAP) tool (Puillandre, Brouillet & Achaz, 2019; https://bioinfo.mnhn.fr/abi/public/asap/; accessed 6 October 2021), using the default settings. The null hypothesis was that only one species exists.

Because no incongruence between the nuclear and plastid markers for the studied taxa was found earlier (Hedenäs & Eldenäs, 2007, 2008), we analysed all molecular data in combination. Since reticulation occurs in *H. vernicosus s.l.* (Hedenäs & Eldenäs, 2007; Hedenäs, 2018), we evaluated relationships between the entities with the outgroups included in NeighborNet Split Networks, produced in SplitsTree v.4.12.6 (Huson & Bryant, 2006). We tested potential support for lineages in a tree context by jacknife analyses (1000 replications) performed with the program TNT (Goloboff, Farris & Nixon, 2003). For the specimens of *H. vernicosus s.l.*, we used the program TCS (Clement, Posada & Crandall, 2000) to identify haplotypes and their relations to each other. Specimens for which only one or two of the molecular markers could be generated were referred to either of the two cryptic species based on their available sequences but were not included in the haplotype analyses. We used the program GENALEX v.6.5 (Peakall & Smouse, 2006,

2012) to estimate haplotype diversity, as the effective number of haplotypes (Ne) and haplotype diversity (*H*), and to estimate pairwise Φ_{PT} (an analogue of F_{ST}, i.e. genetic diversity among populations) by analysis of molecular variance (AMOVA). We used Arlequin v.3.5.2.2 (Excoffier & Lischer, 2010) to calculate nucleotide diversity (π) in the two cryptic species. Our null hypothesis is that no differences exist between the cryptic species. We employed Tajima's *D* test of selective neutrality (Tajima, 1989) to estimate whether European populations of the cryptic species are stable in size or potentially expanding or decreasing. [Tajima's *D* test was preferred over Fu's FS test (Fu, 1997), because it has been shown that the latter should not be used when recombination levels are unknown (Ramírez-Soriano *et al.*, 2008).] Tajima's *D* test was run in Arlequin.

After the geographical distributions of CRS1 and CRS2 were clarified, their distribution patterns suggested different potential post-glacial immigration routes according to Kyrkjeeide *et al.* (2014). Populations in or close to glacial refugial areas are assumed to display higher genetic diversity than populations from areas to which the species have recently spread (cf. Kyrkjeeide *et al.*, 2014). Considering the known patterns of southern refugia for species with relatively southern geographical distributions and eastern or north-eastern refugia for species with more northern distributions (Taberlet *et al.*, 1998; Tollefsrud *et al.*, 2008; Kyrkjeeide *et al.*, 2014), we divided the samples of CRS1 into southern (S population; *N* = 43) and northern (N population; 49) specimen subsets and CRS2 into eastern (E population; 47) and western (W population; 60) subsets, putting the geographical limits so that within each cryptic species both subsets included approximately the same number of specimens. We explored patterns of haplotype diversity (Ne, *H*) and variation (pairwise Φ_{PT}) between the S and N populations of CRS1 and E and W populations of CRS2, respectively, using GENALEX v.6.5. Specimens belonging to these respective subsets are indicated in Figure 1 and Appendix 1.

HABITAT AND CLIMATE PREFERENCES

Potential differences in EC and/or pH values in the water surrounding the mosses were tested, based on 151 samples for CRS1, 73 samples for CRS2 and 20 samples for localities with the two cryptic species together. For CRS1, three samples were collected in Sweden, 127 in the Czech Republic, 11 in the Netherlands, six in Switzerland and five in Spain. For CRS2, 54 samples were collected in Sweden, nine in the Czech Republic, one in Switzerland and nine in Minnesota, USA. Data were derived from Hedenäs & Kooijman (1996), Hedenäs & Eldenäs (2007),
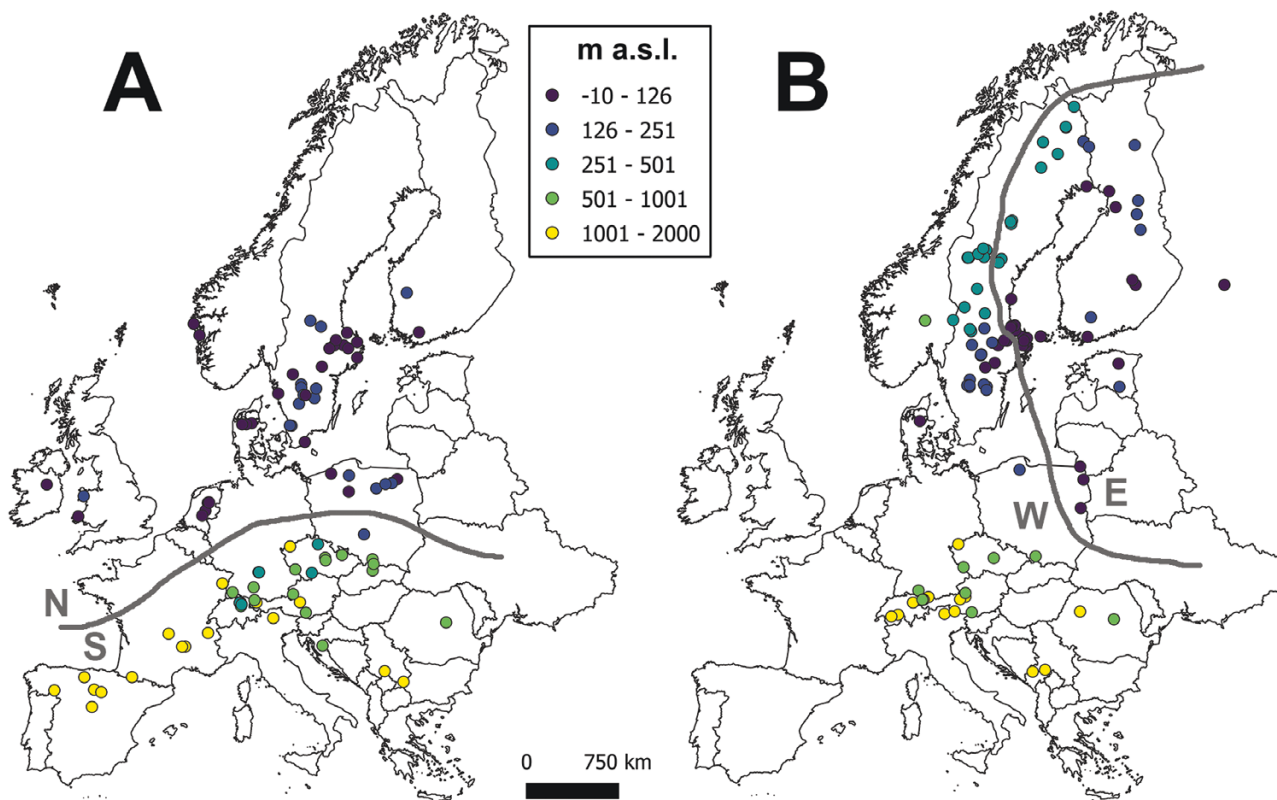
Figure 1. European distributions of cryptic species 1 (A) and 2 (B). The elevation spans, in m a.s.l., of the sampled localities are indicated by different colours. The subdivisions into northern (N) and southern (S) populations in cryptic species 1 (A) and western (W) and eastern (E) populations in cryptic species 2 (B) are indicated by grey lines.

Štechová, Kučera & Šmilauer (2012) and Kooijman *et al.* (2020) and from unpublished records of Lars Hedenäs and Annemieke Kooijman (Sweden), Alžběta Manukjanová and Táňa Štechová (Czech Republic) and Patxi Heras and Marta Infante (Spain). For 134 samples, more elaborate analyses were available in addition to pH and EC, such as Ca, Fe, $N-NO_3$, $N-NH_4$ and/or $P-PO_4$ content of the water (33 from Sweden, 85 from the Czech Republic, 11 from the Netherlands and five from Spain). As additional variables, molar ratios of Ca:Fe, the total amount of inorganic N and the contribution of $N-NH_4$ to total mineral N were calculated. Two records for CRS1 in the Czech Republic contained extreme values for Fe or $N–NO_3$ and were therefore discarded for these parameters. We tested for differences between the cryptic species of *H. vernicosus* with one-factor general linear models with cryptic species (CRS1, CRS2 and CRS1+CRS2) as the independent variable (Cody & Smith, 1987). We also used one-factor general linear models with the six countries as independent factors to test differences between them, and two-factor general linear models to test interactions between cryptic species (only CRS1 and CRS2) and countries. Correlations between

individual habitat characteristics were tested with Pearson correlation tests.

We tested for differences in elevation distribution of the two cryptic species both for all samples and for the samples from regions where both cryptic species occur. We used the Mann–Whitney *U*-test because Shapiro–Wilk *W* was significant and the distributions of the residuals in a preliminary ANOVA were non-normal.

To test the difference between climatic niches, ten climatic variables at 1-km resolution were downloaded from CHELSA v.1.2 or derived from monthly exCHELSA data v.1.2 (see Appendix 2; Karger *et al.*, 2017, 2018). A principal component analysis was computed with these ten variables across the studied area [EPSG 4326; extent: –10°, 42°, 35°, 72° (x_{min}, x_{max}, y_{min}, y_{max})] in R v.4.0.2 (R-Core-Team, 2019) via the modEvA package (Barbosa *et al.*, 2013). The first two principal components, representing 62.93% of the total variance, were kept. For this analysis, the cryptic species occurrences were spatially filtered via the 'dismo' package (Hijmans *et al.*, 2017) to have only one occurrence per pixel of a 1-km resolution map. As niche conservatism or divergence should be tested only within environmental conditions available for the

two cryptic species (Guisan *et al.*, 2014; Qiao, Escobar & Peterson, 2017; Collart *et al.*, 2021), we conducted a multivariate environmental similarity (MESS) analysis (Elith, Kearney & Phillips, 2010) via the 'modEvA' package (Barbosa *et al.*, 2013). We thus only retained occurrences where climates were analogous, reducing the risk of spurious conclusions by removing the geographical influence (i.e. climatic areas that are not accessible for one cryptic species due to, notably, dispersal limitations) and therefore focusing only on potential differences in environmental niches (Guisan *et al.*, 2014; Qiao *et al.*, 2017). With the two principal climatic components and the filtered species data, we computed niche overlaps among the two cryptic species with Schoener's *D* and a modified Hellinger's *I* metric (Warren, Glor & Turelli, 2008) from the 'ecospat' package (Di Cola *et al.*, 2017; Broennimann, Di Cola & Guisan, 2020). Two tests have been developed to determine whether niches are equivalent (equivalency test) or more/less similar than random (similarity test; Warren *et al.*, 2008). However, the equivalency test tends to excessively reject the null hypothesis of niche identity (Peterson, 2011; Broennimann *et al.*, 2012). Consequently, we decided to focus only on the niche similarity test, which was realized following Broennimann *et al.* (2012). The niche similarity test compares the climatic niche overlap between CRS1 and CRS2, to a null distribution of niche overlap inferred from the climatic niche of CRS1 and a climatic niche acquired by randomly relocating the whole observed frequency of occurrences of CRS2 among the available climate in the study area. This computation is reiterated 999 times in each direction (CRS1 to CRS2, or CRS2 to CRS1) to generate the null distribution of random niche overlaps. If the observed niche overlap falls within the 95% confidence limits of the null distribution, the null hypothesis cannot be rejected (Broennimann *et al.*, 2012; Collart *et al.*, 2021). We tested the hypothesis that the cryptic species niches are less similar than expected by chance (observed niche overlap is lower than random), indicating a niche divergence, using the 'ecospat' package (Di Cola *et al.*, 2017; Broennimann *et al.*, 2020). A test of the opposite hypothesis, suggesting a niche conservatism was also carried out.

RESULTS

MOLECULAR ANALYSES

The total number of aligned sites in the studied 217 specimens of *H. vernicosus* and four outgroup specimens, after deletion of regions at the beginning and end of the sequences that were incomplete for some specimens, was 678 for ITS, including 44 base substitutions (seven in *H. vernicosus*), of which 24 (four) were potentially parsimony informative and 11 indels (two), including three (one) potentially informative. The equivalent numbers for *rpl16 and trnL–trnF* were 636 [24 (six), 11 (two), eight (one), seven (one)] and 438 [11 (one), eight (one), one (zero), zero (zero)], respectively.

The ASAP analysis suggested that two statistically supported groups of specimens exist (*P* = 0.0184), corresponding with the two cryptic species CRS1 and CRS2. The NeighborNet revealed the two cryptic species of *H. vernicosus* and *H. lapponicus* as three separate entities (Fig. 2A). *Hamatocaulis* is highly distinct from species of *Scorpidium* (Schimp.) Limpr. (jackknife support 100), and *H. vernicosus* CRS2 is well distinguished from CRS1 and *H. lapponicus* (89). *Hamatocaulis vernicosus* samples with all three markers available yield a TCS network divided into two groups separated by five mutational steps, corresponding to CRS1 and CRS2 (Fig. 2B). The molecular diversity was higher in CRS1 than in CRS2, and Tajima's *D* was significantly negative for both species (Table 1A). Fifty-nine percent of the total molecular variation in *H. vernicosus s.l.* is due to variation between the cryptic species and 41% refers to variation within the cryptic species (Table 1B).

The two cryptic species are sympatric from Central Europe and the Balkans to southern Scandinavia (Fig. 1). Only CRS1 was found in the west and south-west, from western Norway to the Iberian Peninsula (Fig. 1A), and only CRS2 was found in the boreal zone, except for a few localities in the southernmost portion of this zone (Fig. 1B). No or only minor (CRS1) differences in haplotype diversity were found between S and N populations of CRS1 and between E and W populations of CRS2 (Table 2A; specimens belonging to either subset as indicated in Fig. 1 and Appendix 1), and no differences in haplotype composition were found between the S and N subsets of CRS1 (Table B) and E and W subsets of CRS2 (Table 2C). The geographical distributions of the haplotypes of CRS1 and CRS2 are shown in Figure 2C.

HABITAT AND CLIMATE PREFERENCES

The two cryptic species only slightly differed in habitat characteristics related to water chemistry (Tables 3, 4). In the overall analysis, CRS1 showed slightly lower pH values than CRS2, with mean values of 6.3 and 6.6, respectively. These differences were mainly due to imbalances in the dataset with respect to countries (Table 3). CRS1 predominated in the Czech Republic, the Netherlands, Switzerland and Spain, with relatively low pH values. In contrast, CRS2 predominated in Sweden and Minnesota, which showed significantly

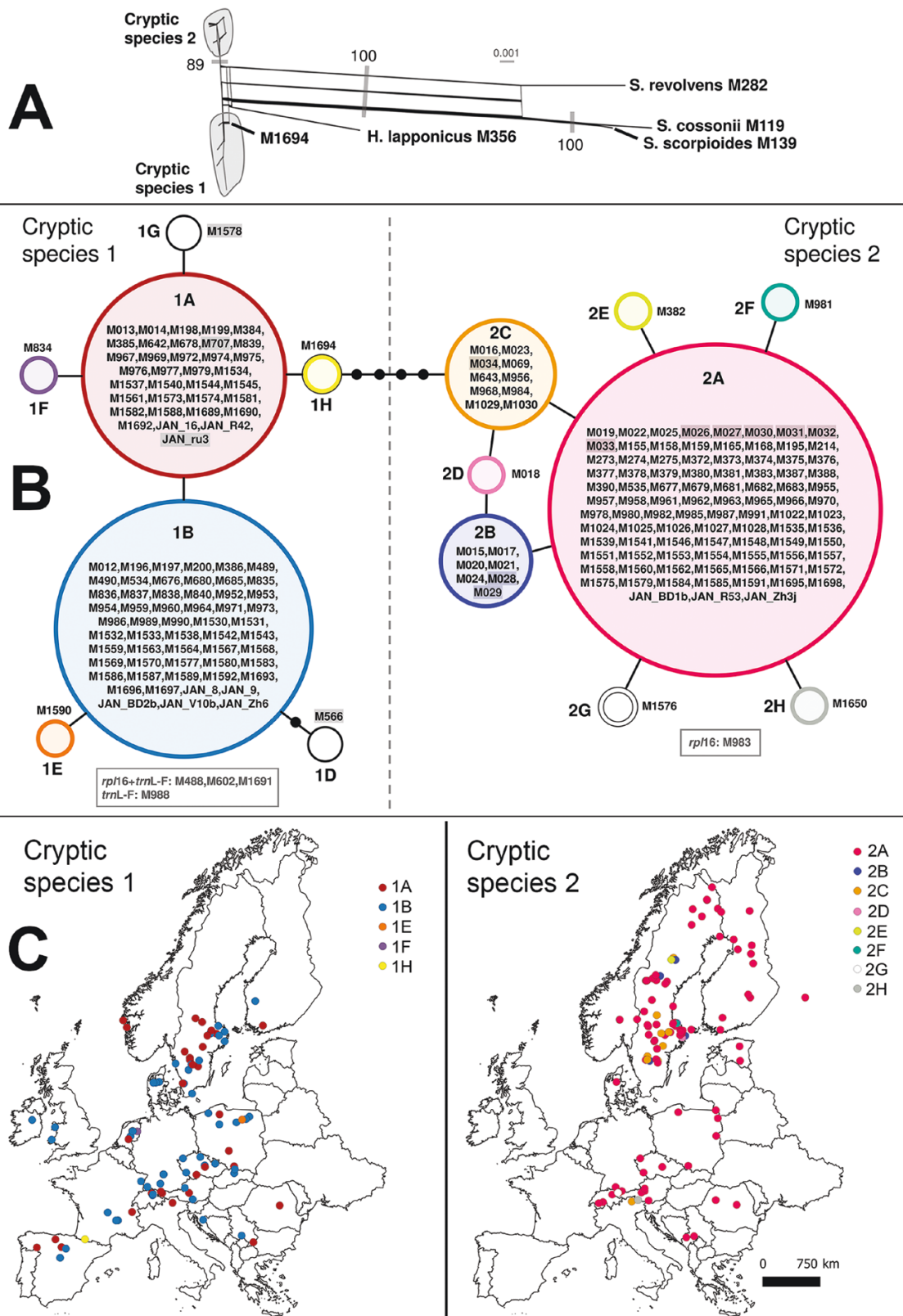**Figure 2.** A, NeighborNet split network, based on ITS, *rpl16* and *trnL–trnF* combined, for *Hamatocaulis vernicosus s.l.* with three *Scorpidium* spp. and *H. lapponicus* as outgroups. Jacknife support > 75 is indicated by grey lines and support

Table 1. Haplotype and nucleotide diversity, Tajima's *D* and the partition of haplotype diversity between the two cryptic species of *Hamatocaulis vernicosus* in Europe, based on ITS, *rpl16* and *trnL–trnF* combined. Indel information was included to define haplotypes, but not to calculate nucleotide diversity. A, Haplotype and nucleotide diversity indices and Tajima's *D*. *N* = number of samples; Na = number of haplotypes; Ne = effective number of haplotypes; *H* = haplotype diversity; π = nucleotide diversity (SD = standard deviation). An asterisk (*) indicates a significant Tajima's *D* ($P < 0.05$). B, Results of AMOVA to partition haplotype variation within and between the two cryptic species. ($N = 199$; 13 haplotypes; $\Phi = 0.593$, $P = 0.0001$, based on 9999 permutations). d.f. = degrees of freedom, SS = sums of squares and MS = mean squared deviations

A

Pop	*N*	Na	Ne	*H*	π (SD)	Tajima's *D*
Cryptic species 1	92	5	2.002	0.500	0.000311 (0.000288)	−1.62025*
Cryptic species 2	107	8	1.458	0.314	0.000203 (0.000221)	−1.53754*

B

Source	d.f.	SS	MS	Estimated % of total	
				Variance	Variation
Between cryptic species	1	29.325	29.325	0.294	59
Within cryptic species	197	39.816	0.202	0.202	41
Total	198	69.141		0.496	100

higher pH values than most other countries. In countries with both cryptic species, such as Sweden and the Czech Republic, pH values did not differ between them. In Switzerland, values for CRS1 were even higher than for CRS2. This means that habitat requirements with respect to pH probably do not differ between CRS1 and CRS2. For EC, the two cryptic species did not differ in the overall analysis, but also not when treated per country. Electrical conductivity could be low for both CRS1 and CRS2, but also reach values of 400–500 µS cm⁻¹. Electrical conductivity significantly correlated with Ca levels ($R = 0.57$), which also did not differ in the overall analysis and showed values between 4 and 68 mg/L Ca for CRS1 and 3–57 mg/L for CRS2. However, Ca concentrations were higher in the Netherlands than in Sweden or the Czech Republic. In the overall analysis, the two cryptic species did not differ in Fe concentrations, although values were generally higher in the Netherlands

than in Sweden or the Czech Republic. *Hamatocaulis vernicosus* is known for its tolerance to Fe-rich habitats, and high Fe concentrations were found for both cryptic species. For both CRS1 and CRS2, Fe levels could be close to zero, but also showed values (much) > 20 µmol L⁻¹ or 1.12 mg L⁻¹ in > 25% of the cases. The molar Ca:Fe ratio did not differ between cryptic species in the overall analysis and showed that concentrations were generally higher for Ca than for Fe. High Ca:Fe ratios were especially found in the Netherlands. In the correlation analysis, pH significantly correlated with EC ($R = 0.20$) and Ca ($R = 0.18$), which also correlated with each other ($R = 0.57$). Correlations with Fe were, however, not significant.

With respect to nutrients in the water, the two cryptic species did not differ in N-NO$_3$, N-NH$_4$ and total mineral N concentrations, although the Czech Republic showed relatively high values for nitrate and low values for ammonium (Table 5). The contribution

values. In cryptic species 1, sample M1694, which is molecularly most similar to one haplotype of cryptic species 2 (Fig. 1B), is indicated. B, Haplotype network for the two cryptic species of *Hamatocaulis vernicosus s.l.*, based on ITS, *rpl16* and *trnL–trnF* combined. Circle sizes are proportional to the number of samples (total $N = 212$). For five additional samples, in grey boxes below the network, only one or two of the plastid markers could be retrieved, and their exact haplotype within the respective cryptic species could not be determined. Lines between circles represent one mutational change and the dots on the line between the two cryptic species represent 'missing' haplotypes. Cryptic species 1 includes 96 European and four extra-European [shaded numbers: Russia or Peru (M707)] specimens and cryptic species 2 includes 108 European and nine extra-European (USA: Minnesota) samples. Sample numbers correspond with those in Appendix 1. C, European distributions of the haplotypes that belong to cryptic species 1 and 2.

Table 2. Haplotype diversity and the partition of haplotype diversity between subsets within cryptic species 1 (CRS1) and cryptic species 2 (CRS2) of *Hamatocaulis vernicosus* in Europe, based on ITS, *rpl16* and *trnL–trnF* combined. A, Haplotype diversity indices. N = number of samples; Na = number of haplotypes; Ne = effective number of haplotypes; H = haplotype diversity. B, Results of AMOVA to partition haplotype variation within and between S and N populations of CRS1 (N = 92; 5 haplotypes; Φ = −0.020, P = 0.939, based on 9999 permutations). C, Results of AMOVA to partition haplotype variation within and between E and W populations of CRS2 (N = 107; 8 haplotypes; Φ = −0.009, P = 0.200, based on 9999 permutations). d.f. = degrees of freedom, SS = sums of squares and MS = mean squared deviations

A

Pop	N	Na	Ne	H
CRS1 S population	43	3	1.982	0.504
CRS1 N population	49	4	2.016	0.495
CRS2 E population	47	6	1.369	0.270
CRS2 W population	60	5	1.516	0.341

B

Source	d.f.	SS	MS	Estimated % of total	
				Variance	Variation
Between CRS1 S and N pop.	1	0.024	0.024	0.000	0
Within CRS1 populations	90	22.998	0.256	0.256	100
Total	91	23.022		0.256	100

C

Source	d.f.	SS	MS	Estimated % of total	
				Variance	Variation
Between CRS2 E and W pop.	1	0.237	0.237	0.002	1
Within CRS2 populations	105	16.557	0.158	0.158	99
Total	106	16.794		0.159	100

of NH$_4$ to total mineral N was higher for CRS2 than CRS1, but this was mainly due to low values in the Czech Republic, in which CRS1 predominated. In Sweden and the Czech Republic, the two cryptic species did not differ. In the overall analysis, P-PO$_4$ concentrations were significantly higher for CRS1 than for CRS2, mainly due to high levels in the Netherlands, in which only CRS1 occurred. In Sweden and the Czech Republic, the two cryptic species did not differ. Correlations between nutrients and other habitat factors were significant to some extent. Total mineral N and N-NH$_4$ positively correlated with the Ca:Fe ratio (R = 0.52 and 0.41, respectively). The contribution of N-NH$_4$ to total mineral N increased with pH (R = 0.28), and P-PO$_4$ positively correlated with Fe (R = 0.36).

No differences were revealed in the elevation distributions for the two cryptic species (Fig. 1) in the total data set (CRS1: mean 459 m a.s.l., N = 96; CRS2: mean 356 m a.s.l., N = 108. Mann–Whitney U-test: U = 4851, Z = 0.790, P = 0.429) or for the samples from

regions where they are sympatric (CRS1: mean 454 m a.s.l., N = 63; CRS2: mean 417 m a.s.l., N = 61. Mann–Whitney U-test, U = 1590, Z = 1.654, P = 0.098).

For environmental niche comparisons, the MESS analysis removed 15 and 17 occurrences, resulting in 72 and 86 occurrences usable for the further analyses, for CRS1 and CRS2, respectively (Appendix 3). The climatic niche overlap was high between the two cryptic species (D = 0.82; I = 0.97). Although the climatic niches were largely overlapping, the niche similarity test did not confirm a niche conservatism (P = 0.156 and 0.147 for D and I niche overlap metrics, respectively; see Appendix 4) or a niche divergence (P = 0.858 and 0.863 for D and I metrics).

DISCUSSION

We found no differences in habitat or climate parameters that could explain the different distributions of the genetically well separated CRS1

Table 3. Habitat factors pH and electrical conductivity (EC) of the water surrounding the cryptic species 1 and 2 of *Hamatocaulis vernicosus* in different countries. Values given are mean values and standard deviations. Differences between countries and cryptic species were tested with two-factor general linear models; different letters indicate significant differences in pH or EC ($P < 0.05$) between particular mean values for a cryptic species in a particular country

Habitat factor	Country	n	Cryptic species 1	Cryptic species 2
pH	Sweden	57	6.8 (0.6) [ab]	6.6 (0.5) [ab]
	Czech Republic	156	6.3 (0.5) [cd]	6.3 (0.3) [bc]
	Netherlands	11	6.1 (0.) [a]	-
	Switzerland	6	6.7 (0.7) [bc]	5.4 (-) [a]
	Spain	5	6.1 (0.6) [a]	-
	USA (Minnesota)	9	-	7.1 (0.5) [d]
EC	Sweden	57	138 (80) [a]	127 (81) [a]
(μS cm^{-1})	Czech Republic	129	156 (125) [a]	165 (182) [a]
	Netherlands	11	296 (131) [b]	-
	Switzerland	6	129 (89) [a]	18 (-) [a]
	Spain	5	58 (32) [a]	-
	USA (Minnesota)	9	-	314 (125) [b]

Table 4. Concentrations of Ca and Fe and Ca:Fe ratios of the water surrounding the cryptic species 1 and 2 of *Hamatocaulis vernicosus* in different countries. Values given are mean values and standard deviations. Differences between countries and cryptic species were tested with two-factor general linear models; different letters indicate significant differences ($P < 0.05$) between particular mean values for a cryptic species in a particular country

Habitat factor	Country	n	Cryptic species 1	Cryptic species 2
Ca (mg L^{-1})	Sweden	33	11 (3) [a]	23 (14) [a]
	Czech Republic	85	17 (12) [a]	25 (30) [ab]
	Netherlands	11	35 (17) [b]	-
Fe	Sweden	33	5.3 (4.0) [ab]	3.0 (3.5) [a]
(mg L^{-1})	Czech Republic	83	2.3 (5.8) [a]	0.6 (0.1) [ab]
	Netherlands	11	9.7 (15.2) [b]	-
Ca:Fe	Sweden	33	7 (8) [a]	70 (115) [ab]
(mol mol^{-1})	Czech Republic	83	50 (107) [a]	69 (8) [ab]
	Netherlands	11	155 (213) [b]	-

and CRS2 of *H. vernicosus* in western and central Europe. Neither did we find regional intraspecific molecular differentiation within the two cryptic species that could have correlated with hypotheses of post-glacial immigration of CRS1 from refugia in southern Europe and of CRS2 from the east or north-east. A significant negative Tajima's *D* for both cryptic species at the European level suggests that both are presently increasing. This could possibly be due to colonization of wetlands that gradually became available due to expanding agricultural management over thousands of years.

MOLECULAR RELATIONSHIPS

The significant split into two groups in the ASAP analysis (Puillandre *et al.*, 2019) confirms that CRS1

and CRS2 are well differentiated molecularly. In combination with the non-existent exchange of genetic material between them (Fig. 2B, and Hedenäs & Eldenäs, 2007; Hedenäs, 2018; Manukjanová, Košnar & Kučera, 2020), the closer relationship of CRS1 to *H. lapponicus* than to CRS2 (Fig. 2A) and the different geographical distributions in Europe (Fig. 1), this shows that they behave in all respects as species. In view of the lack of morphological differentiation, they should therefore be treated as cryptic species. Cryptic species are sometimes formally described among other organisms, but this has not yet become the practice for bryophytes (Wagner & Wagner Jr., 1989; Heinrichs *et al.*, 2011; Hedenäs, 2020a, b). Among the problems listed in these two studies, knowing which cryptic species the type specimen belongs to is perhaps the most crucial for *H. vernicosus*. The type of *Stereodon*

Table 5. Nutrient concentrations (µg L^{-1}) of the water surrounding the cryptic species 1 and 2 of *Hamatocaulis vernicosus* in different countries. Values given are mean values and standard deviations. Different letters indicate significant differences in N-NO$_3$ concentrations ($P < 0.05$) between particular mean values for a cryptic species in a particular country.

Habitat factor	Country	n	Cryptic species 1	Cryptic species 2
N-NO$_3$	Sweden	33	30 (47) [ab]	30 (33) [a]
(µg L^{-1})	Czech Republic	75	108 (176) [b]	142 (130) [ab]
	Netherlands	11	17 (13) [a]	-
N-NH$_4$	Sweden	33	314 (435) [ab]	236 (295) [a]
(µg L^{-1})	Czech Republic	76	173 (465) [a]	135 (42) [a]
	Netherlands	11	267 (375) [a]	-
	Spain	5	740 (343) [b]	-
Total mineral N	Sweden	33	343 (483) [a]	265 (293) [a]
(µg L^{-1})	Czech Republic	75	326 (587) [a]	277 (88) [a]
	Netherlands	11	284 (382) [a]	-
Contribution N-NH$_4$	Sweden	33	94 (5) [b]	78 (24) [b]
(% total mineral N)	Czech Republic	75	58 (30) [a]	54 (33) [ab]
	Netherlands	11	87 (9) [b]	-
P-PO$_4$	Sweden	33	7 (3) [a]	9 (11) [a]
(µg L^{-1})	Czech Republic	76	13 (7) [a]	13 (3) [a]
	Netherlands	11	39 (41) [b]	-

vernicosus Mitt., the basionym of *H. vernicosus*, was collected 1858 in a now destroyed wetland situated in a region where both CRS1 and CRS2 occurred. The cryptic species to which the type belongs can therefore not be established.

In CRS1, the two main haplotypes are about equally frequent and evenly distributed in Europe (cf. Fig. 2C and Appendix 1), whereas in CRS2 one haplotype is dominant. This causes a higher haplotype diversity in CRS1 than in CRS2 (and a similar difference in nucleotide diversity), in line with results from the Czech Republic (Manukjanová *et al.*, 2020), but not from Sweden where the two cryptic species display equal diversity (Hedenäs, 2018). The situation in Sweden could be a result of smaller populations and presumably smaller effective population sizes (Ellegren & Galtier, 2016) of CRS1 than of CRS2 in Sweden, where CRS1 is restricted to the southern third of the country, whereas CRS2 occurs throughout the country. The geographically restricted sampling of Hedenäs (2018), from regions with relatively abundant and also relatively undisturbed wetlands where the *H. vernicosus* populations are probably more stable than elsewhere in Europe, could also explain why Tajima's *D* was not significant in that study, whereas it was significantly negative for both cryptic species in the present study. The similarly negative Tajima's *D* for both CRS1 and CRS2 could indicate that large portions of their European populations are presently expanding after an earlier bottleneck. We believe it is unlikely that both cryptic species should display Tajima's *D* of similar negative magnitudes due to other potential factors, such as recent selective sweeps or

purifying selection (Simonsen, Churchill & Aquadro, 1995). A possible explanation is that the expansion of *H. vernicosus s.l.* after the glacial bottleneck finished early in Scandinavia, whereas the expansion at the European level reflects that many localities south of Scandinavia gradually became suitable only relatively recently. This could be a result of the gradual implementation of extensive agricultural management of wetlands over most of the continent during a period of > 6000 years (Joosten & Tanneberger, 2017), including grazing and hay harvest that promote less competitive plants such as bryophytes (Bergamini *et al.*, 2001; Singh *et al.*, 2021).

HOW TO EXPLAIN THE DISTRIBUTIONS OF THE CRYPTIC SPECIES

Only CRS1 was sampled in westernmost/south-westernmost Europe, and only CRS2 was found in northern Fennoscandia, whereas they are sympatric in the other studied regions (Fig. 1). Such clear differences in geographical distributions beg for an explanation, which can be either in terms of different habitat preferences or immigration histories.

The two cryptic species did not really differ in habitat conditions, although their ranges could differ between countries. In agreement with Štechová *et al.* (2012), both cryptic species grow in mineral-rich habitats with neutral pH. Electric conductivity and Ca levels were strongly correlated and varied for both cryptic species in a similar way. For nutrients such as N and P, the levels were generally rather low, except for some Fe-rich fens in the Netherlands, which helps

reduce the growth of vascular plants and increase the density of *H. vernicosus* (Štechová *et al.*, 2012). The most characteristic habitat factor for *H. vernicosus s.l.* is probably the tolerance to high Fe. This taxon is thought to be more Fe-tolerant than other brown mosses such as *Scorpidium scorpioides* (Hedenäs & Kooijman, 1996; Mettrop *et al.*, 2018). Both cryptic species of *H. vernicosus* were found over a wide range of Fe concentrations in the water, including values above the high and very high levels of 20 and 200 µmol L^{-1} of Vicherová, Hájek & Hájek (2015) or 1.12 and 11.2 mg L^{-1}. Aggenbach *et al.* (2013) indicated that *H. vernicosus* did not occur in fens with Fe concentrations >56 mg L^{-1}, but they compared pristine fens with heavily degraded fens in which typical mosses may have been absent for other reasons, such as high aboveground biomass. In our study, *H. vernicosus* was found even at 152 mg Fe L^{-1}. The populations of *H. vernicosus* are usually more extensive under Fe-rich conditions (Štechová *et al.*, 2012). This may be due to Fe toxicity to vascular plants, or low relative growth rates for Fe-tolerant species (Wheeler, Al-Farraj & Cook, 1985; Snowden & Wheeler, 1993, 1995), which both reduce aboveground biomass. On the other hand, both cryptic species may profit from the relatively high P-PO$_4$ concentrations in Fe-rich fens, which positively correlated with each other, in agreement with Kooijman *et al.* (2020). However, *H. vernicosus* may only be tolerant to high Fe levels as long as pH is relatively high (Vicherová *et al.*, 2015). The latter showed that CRS1 could grow even at 200 µmol Fe L^{-1} or 11.2 mg Fe L^{-1}, as long as pH was kept at *c*. 7.1 and Ca was also supplied. For this reason, it is important that the molar Ca:Fe ratio was (far) > 1 for all samples, except for the most Fe-rich locality in the Czech Republic. No experiments have been performed to test tolerance to high Fe levels for CRS2, but the overlap in habitat characteristics related to Fe, pH and Ca suggest that this characteristic has developed before the separation of the two clades. This also means that both cryptic species are sensitive to acidification of their habitats, which is a major threat to this species.

Neither this study nor Manukjanová *et al.* (2019a) found differences in elevation distributions between the two cryptic species, and our results show that the climatic niche overlap between the two is high, and neither climatic niche conservatism nor niche divergence could be confirmed. CRS1, which in Europe is the southern cryptic species, also occurs in Arctic Russia (M566, M1578; Appendix 1) and can thus grow in very cold climates. This suggests that CRS1 and CRS2 are likely to share similar climate preferences. The lack of niche differentiation along the investigated habitat, elevation and climate parameters suggest that other factors explain the different distributions of the two cryptic species. Both cryptic species are widespread outside Europe. Although their extra-European distributions are known only from scattered samples (CRS1: Buryatia, Taimyr and Wrangel Island; CRS2: Minnesota), their distributions probably cover large portions of the Northern Hemisphere, with outliers in the south for at least CRS1 (Peru). The existence of 1.8–2.6 Myr-old finds of the morphology-defined species (Hedenäs & Bennike, 2008), suggests that the species, and probably the two cryptic species, attained their wide distributions long before the last glacial period. However, to explain the global history of the two cryptic species a much wider sampling than we have at present is required. For Europe, one important factor to explain phylogeographic patterns in species is their glacial and post-glacial histories (e.g. Taberlet *et al.*, 1998; Svenning & Skov, 2007; Parducci *et al.*, 2012; Kyrkjeeide *et al.*, 2014). Kyrkjeeide *et al.* (2014) suggested three main post-glacial colonization routes for European bryophytes, the western, southern and eastern routes. Based on total geographical distributions only, that of CRS1 seems to fit elegantly into their southern route, implying that it survived the Last Glacial Maximum (LGM *c.* 30–16 kA BP) in the Iberian, Italian and Balkan Peninsulas and that it has not yet reached the northern portions of Europe. CSR2 equally well fits their eastern route, implying that it survived the LGM east of glaciated Europe and has not yet reached the western and south-western regions of this continent. We did not find a higher genetic diversity or different genetic composition in subsets of specimens sampled closer to the supposed refugial regions than further away, as could be expected under these scenarios (cf. Kyrkjeeide *et al.*, 2014) and the distributions of the individual haplotypes (Fig. 2C) did not suggest distinct geographical patterns. Thus, unlike for some well-studied European bryophytes, such as *Leucodon sciuroides* (Hedw.) Schwägr. (Cronberg, 2000), *Rhytidium rugosum* (Hedw.) Kindb. (Hedenäs, 2015) and *Sanionia uncinata* (Hedw.) Loeske (Hedenäs, 2010), but in common with other species (Kyrkjeeide *et al.*, 2014), the variation in the studied molecular markers does not provide additional evidence regarding the post-glacial origin of each of the cryptic species within *H. vernicosus*. The two cryptic species within *H. vernicosus* inhabit narrower habitats than the three mentioned bryophyte species, suggesting that their refugial populations could potentially have been smaller and therefore experienced stronger bottleneck effects. This would have resulted in low overall remaining genetic variation that is insufficient to reveal patterns related to dispersal history.

CONCLUSIONS

Hamatocaulis vernicosus was placed on the EU Habitat Directive Appendix II to protect it and to ensure its

long-term survival in the European Union. This led to a multitude of actions to determine its actual frequency and measures for its survival. The revelation that it includes two cryptic species complicates the situation, since each of these is necessarily rarer than the original morphology-defined species. We here show that: (1) the two cryptic species have partly different geographical distributions in western Europe: (2) the western European populations of both have genetic signs of a slight increase, possibly connected with a long-term increase linked with the spread of agricultural practices in wetlands over thousands of years, (3) the two cryptic species occur under similar chemical and climatic conditions and (4) the post-glacial origins hypothesized here, suggested by the distribution patterns of the respective cryptic species, are not accompanied by corresponding intraspecific genetic differentiation. We therefore suggest that more variable molecular markers are used to test the presented post-glacial immigration hypothesis.

ACKNOWLEDGEMENTS

FUNDING

DATA AVAILBILITY

The data underlying this article are available in the GenBank Nucleotide Database and can be accessed with the accession numbers provided in Appendix 1.

REFERENCES

Aggenbach CJS, **Backx H**, **Emsens WJ**, **Grootjans AP**, **Lamers LPM**, **Smolders AJP**, **Stuyfzand PJ**, **Wołejko L**, **Van Diggelen R. 2013.** Do high iron concentrations in rewetted rich fens hamper restoration? *Preslia* **85:** 405–420.

Anonymous. **1992.** Council Directive 92/43/EEC of 21 May 1992 on the conservation of natural habitats and of wild fauna and flora. *Official Journal of the European Communities* **L206:** 7–50.

Barbosa AM, **Real R**, **Muñoz A-R**, **Brown JA. 2013.** New measures for assessing model equilibrium and prediction mismatch in species distribution models. *Diversity and Distributions* **19:** 1333–1338.

Bergamini A, **Peintinger M**, **Schmid B**, **Urmi E. 2001.** Effects of management and altitude on bryophyte species diversity and composition in montane calcareous fens. *Flora* **196:** 180–193.

Bickford D, **Lohman DJ**, **Sodhi NS**, **Ng PKL**, **Meier R**, **Winker K**, **Ingram KK**, **Das I. 2006.** Cryptic species as a window on diversity and conservation. *Trends in Ecology and Evolution* **22:** 148–155.

Broennimann O, **Di Cola V**, **Guisan A. 2020.** ecospat: spatial ecology miscellaneous methods. R package version 3.1. Available at: https://CRAN.R-project.org/package=ecospat.

Broennimann O, **Fitzpatrick MC**, **Pearman PB**, **Petitpierre B**, **Pellisier L**, **Yoccoz NG**, **Thuiller W**, **Fortin M-J**, **Randin C**, **Zimmermann NE**, **Graham CH**, **Guisan A. 2012.** Measuring ecological niche overlap from occurrence and spatial environmental data. *Global Ecology and Biogeography* **21:** 481–497.

Clement M, **Posada D**, **Crandall KA. 2000.** TCS: a computer program to estimate gene genealogies. *Molecular Ecology* **9:** 1657–1659.

Cody RP, **Smith JK**, **1987.** *Applied statistics and the SAS programming language*, *2nd edn*. Amsterdam: North-Holland Publishing.

Collart F, **Hedenäs L**, **Broennimann O**, **Guisan A**, **Vanderpoorten A. 2021.** Intraspecific differentiation: implications for niche and distribution modelling. *Journal of Biogeography* **48:** 415–426.

Cronberg N. 2000. Genetic diversity of the epiphytic bryophyte *Leucodon sciuroides* in formerly glaciated versus nonglaciated parts of Europe. *Heredity* **84:** 710–720.

Di Cola V, **Broennimann O**, **Petitpierre B**, **Breiner FT**, **D'Amen M**, **Randin C**, **Engler R**, **Pottier J**, **Pio D**, **Dubuis A**, **Pellisier L**, **Mateo RG**, **Hordijk W**, **Salamin N**, **Guisan A. 2017.** ecospat: an R package to support spatial analyses and modeling of species niches and distributions. *Ecography* **40:** 774–787.

Elith J, **Kearney M**, **Phillips S. 2010.** The art of modelling range-shifting species. *Methods in Ecology and Evolution* **1:** 330–342.

Ellegren H, **Galtier N. 2016.** Determinants of genetic diversity. *Nature Reviews Genetics* **17:** 422–433.

Excoffier L, **Lischer HEL. 2010.** Arlequin suite ver 3.5: a new series of programs to perform population genetics analyses under Linux and Windows. *Molecular Ecology Resources* **10:** 564–567.

Feliner GN, **Rosselló JA. 2007.** Better the devil you know? Guidelines for insightful utilization of nrDNA ITS in species-level evolutionary studies in plants. *Molecular Phylogenetics and Evolution* **44:** 911–919.

Fu Y. 1997. Statistical tests of neutrality of mutations against population growth, hitchhiking and background selection. *Genetics* **147:** 915–925.

Goloboff P, **Farris J**, **Nixon K. 2003.** Tree analysis using new technology. Available at: http://www.lillo.org.ar/phylogeny/tnt/, accessed 3 May 2017.

Graham J, **Farr G**, **Hedenäs L**, **Devez A**, **Watts MJ. 2019.** Using water chemistry to define ecological preferences within the moss genus *Scorpidium*, from Wales, UK. *Journal of Bryology* **41:** 197–204.

Guisan A, **Petitpierre B**, **Broennimann O**, **Daehler C**, **Kueffer C. 2014.** Unifying niche shift studies: insights from biological invasions. *Trends in Ecology and Evolution* **29:** 260–269.

Hedenäs L. 2003. The European species of the *Calliergon-Scorpidium-Drepanocladus* complex, including some related or similar species. *Meylania* **28:** 1–116.

Hedenäs L. 2010. Phylogeography and origin of European *Sanionia uncinata* (Amblystegiaceae, Bryophyta). *Systematics and Biodiversity* **8:** 177–191.

Hedenäs L. 2015. *Rhytidium rugosum* (Bryophyta) colonized Scandinavia from at least two glacial refugial source populations. *Botanical Journal of the Linnean Society* **179:** 635–657.

Hedenäs L. 2016. Intraspecific diversity matters in bryophyte conservation - internal transcribed spacer and *rpl16* G2 intron variation in European mosses. *Journal of Bryology* **38:** 173–182.

Hedenäs L. 2018. Conservation status of the two cryptic species of *Hamatocaulis vernicosus* (Bryophyta) in Sweden. *Journal of Bryology* **40:** 307–315.

Hedenäs L. 2019. On the frequency of northern and mountain genetic variants of widespread species: essential biodiversity information in a warmer world. *Botanical Journal of the Linnean Society* **191:** 440–474.

Hedenäs L. 2020a. Cryptic and morphologically recognizable species diversity within Scandinavian *Plagiopus oederianus* (Bryophyta: Bartramiaceae). *Lindbergia* **43:** linbg.01130.

Hedenäs L. 2020b. Cryptic speciation revealed in Scandinavian *Racomitrium lanuginosum* (Hedw.) Brid. (Grimmiaceae). *Journal of Bryology* **42:** 117–127.

Hedenäs L, **Bennike O. 2008.** A Plio-Pleistocene moss assemblage from Store Koldewey, NE Greenland. *Lindbergia* **33:** 23–37.

Hedenäs L, **Eldenäs P. 2007.** Cryptic speciation, habitat differentiation, and geography in *Hamatocaulis vernicosus* (Calliergonaceae, Bryophyta). *Plant Systematics and Evolution* **268:** 131–145.

Hedenäs L, **Eldenäs P. 2008.** Relationships in *Scorpidium* (Calliergonaceae, Bryophyta), especially between *S. cossonii* and *S. scorpioides*. *Taxon* **57:** 121–130.

Hedenäs L, **Heinrichs J**, **Gallego MT. 2019.** The Scandinavian *Syntrichia ruralis* complex (Musci, Pottiaceae): a chaos of diversification. *Plant Systematics and Evolution* **305:** 639–661.

Hedenäs L, **Kooijman A. 1996.** Phylogeny and habitat adaptations within a monophyletic group of wetland moss genera (Amblystegiaceae). *Plant Systematics and Evolution* **199:** 33–52.

Heinrichs J, **Hentschel J**, **Feldberg K**, **Bombosch A**, **Schneider H. 2009.** Phylogenetic biogeography and taxonomy of disjunctly distributed bryophytes. *Journal of Systematics and Evolution* **47:** 497–508.

Heinrichs J, **Kreier H-P**, **Feldberg K**, **Schmidt AR**, **Zhu R-L**, **Shaw B**, **Shaw AJ**, **Wisseman V. 2011.** Formalizing morphologically cryptic biological entities: new insights from DNA taxonomy, hybridization, and biogeography in the leafy liverwort *Porella platyphylla* (Jungermanniopsida, Porellales). *American Journal of Botany* **98:** 1252–1262.

Hijmans RR, **Phillips S**, **Leathwick J**, **Elith J. 2017.** dismo: species distribution modeling. R package version 1.1-4. Available at: https://CRAN.R-project.org/package=dismo.

Hodgetts N, **Cálix M**, **Englefield E**, **Fettes N**, **García Criado M**, **Patin L**, **Nieto A**, **Bergamini A**, **Bisang I**, **Baisheva E**, **Campisi P**, **Cogoni A**, **Hallingbäck T**, **Konstantinova N**, **Lockhart N**, **Sabovljevic M**, **Schnyder N**, **Schröck C**, **Sérgio C**, **Sim-Sim M**, **Vrba J**, **Ferreira CC**, **Afonina O**, **Blockeel TL**, **Blom H**, **Caspari S**, **Gabriel R**, **Garcia C**, **Garilleti R**, **González Mancebo J**, **Goldberg I**, **Hedenäs L**, **Holyoak D**, **Hugonnot V**, **Huttunen S**, **Ignatov M**, **Ignatova E**, **Infante M**, **Juutinen R**, **Kiebacher T**, **Köckinger H**, **Kučera J**, **Lönnell N**, **Lüth M**, **Martins A**, **Maslovsky O**, **Papp B**, **Porley R**, **Rothero G**, **Söderström L**, **Ştefănuţ S**, **Syrjänen K**, **Untereiner A**, **Váňa J**, **Vanderpoorten A**, **Vellak K**, **Aleffi M**, **Bates J**, **Bell N**, **Brugués M**, **Cronberg N**, **Denyer J**, **Duckett J**, **During HJ**, **Enroth J**, **Fedosov V**, **Flatberg K-I**, **Ganeva A**, **Gorski P**, **Gunnarsson U**, **Hassel K**, **Hespanhol H**, **Hill M**, **Hodd R**, **Hylander K**, **Ingerpuu N**, **Laaka-Lindberg S**, **Lara F**, **Mazimpaka V**, **Mežaka A**, **Müller F**, **Orgaz JD**, **Patiño J**, **Pilkington S**, **Puche F**, **Ros RM**, **Rumsey F**, **Segarra-Moragues JG**, **Seneca A**, **Stebel A**, **Virtanen R**, **Weibull H**, **Wilbraham J**, **Żarnowiec J**, **2019.** *A miniature world in decline: European Red List of mosses, liverworts and hornworts*. Brussels: IUCN.

Huson DH, **Bryant D. 2006.** Application of phylogenetic networks in evolutionary studies. *Molecular Biology and Evolution* **23:** 254–267.

Hutsemékers V, **Hardy OJ**, **Mardulyn P**, **Shaw AJ**, **Vanderpoorten A. 2010.** Macroecological patterns of genetic structure and diversity in the aquatic moss *Platyhypnidium riparioides*. *New Phytologist* **185:** 852–864.

Joosten H, **Tanneberger F. 2017.** Peatland use in Europe. In: Joosten H, Tanneberger F, Moen A eds. *Mires and peatlands of Europe. Status, distribution and conservation*. Stuttgart: Schweizerbart Science Publishers, 151–172.

Karger DN, **Conrad O**, **Böhner J**, **Kawohl T**, **Kreft H**, **Soria-Auza RW**, **Zimmermann NE**, **Linder HP**, **Kessler M. 2017.** Climatologies at high resolution for the earth's land surface areas. *Scientific Data* **4:** 170122.

Karger DN, **Conrad O**, **Böhner J**, **Kawohl T**, **Kreft H**, **Soria-Auza RW**, **Zimmermann NE**, **Linder HP**, **Kessler M. 2018.** Data from: Climatologies at high resolution for the Earth's land surface areas. Available at: https://doi.org/10.5061/dryad.kd1d4.

Kooijman AM, **Cusell C**, **Hedenäs L**, **Lamers LPM**, **Mettrop IS**, **Neijmeijer T. 2020.** Re-assessment of

phosphorus availability in fens with varying contents of iron and calcium. *Plant and Soil* **447:** 219–239.

Košnar J, **Herbstová M**, **Kolář F**, **Koutecký P**, **Kučera J. 2012.** A case of intragenomic ITS variation in bryophytes: assessment of gene flow and role of plyploidy in the origin of European taxa of the *Tortula muralis* (Musci: Pottiaceae) complex. *Taxon* **61:** 709–720.

Kyrkjeeide MO, **Stenøien HK**, **Flatberg KI**, **Hassel K. 2014.** Glacial refugia and post-glacial colonization patterns in European bryophytes. *Lindbergia* **37:** 47–59.

Magdy M, **Werner O**, **McDaniel SF**, **Goffinet B**, **Ros RM. 2016.** Genomic scanning using AFLP to detect loci under selection in the moss *Funaria hygrometrica* along a climate gradient in the Sierra Nevada Mountains, Spain. *Plant Biology* **18:** 280–288.

Manukjanová A, **Košnar J**, **Kučera J. 2020.** Genetic variation in two cryptic species of the rare fen moss *Hamatocaulis vernicosus* in the Czech Republic. *Preslia* **92:** 57–72.

Manukjanová A, **Koutecký P**, **Štechová T**, **Kučera J. 2019a.** Insights into the distribution patterns, habitat and morphologic differentiation of cryptic species of the moss *Hamatocaulis vernicosus* in the Czech Republic. *Herzogia* **32:** 183–199.

Manukjanová A, **Štechová T**, **Kučera J. 2019b.** Expressed sex ratio in populations of the moss *Hamatocaulis vernicosus* (Mitt.) Hedenäs (Scorpidiaceae) in the Czech Republic with consideration of its cryptic species. *Cryptogamie Bryologie* **40:** 41–58.

Mettrop IS, **Neijmeijer T**, **Cusell C**, **Lamers LPM**, **Hedenäs L**, **Kooijman AM. 2018.** Calcium and iron as key drivers of brown moss composition through differential effects on phosphorus availability. *Journal of Bryology* **40:** 350–357.

Mikulášková E, **Hájek M**, **Veleba A**, **Johnson MG**, **Hájek T**, **Shaw JA. 2015.** Local adaptations in bryophytes revisited: the genetic structure of the calci-tolerant peatmoss *Sphagnum warnstorfii* along geographic and pH gradients. *Ecology and Evolution* **5:** 229–242.

Müller K. 2005. SeqState. *Applied Bioinformatics* **4:** 65–69.

Parducci L, **Jørgensen T**, **Tollefsrud MM**, **Elverland E**, **Alm T**, **Fontana SL**, **Bennett KD**, **Haile J**, **Matetovici I**, **Suyama Y**, **Edwards ME**, **Andersen K**, **Rasmussen M**, **Boessenkool S**, **Coissac E**, **Brochmann C**, **Taberlet P**, **Houmark-Nielsen M**, **Larsen NK**, **Orlando L**, **Gilbert MTP**, **Kjær KH**, **Alsos IG**, **Willerslev E. 2012.** Glacial survival of boreal trees in northern Scandinavia. *Science* **335:** 1083–1086.

Patiño J, **Vanderpoorten A. 2018.** Bryophyte biogeography. *Critical Reviews in Plant Science* **37:** 175–209.

Peakall R, **Smouse PE. 2006.** GENALEX 6: genetic analysis in Excel. Population genetic software for teaching and research. *Molecular Ecology Notes* **6:** 288–295.

Peakall R, **Smouse PE. 2012.** GenAlEx 6.5: genetic analysis in Excel. Population genetic software for teaching and research – an update. *Bioinformatics* **28:** 2537–2539.

Pearman PB, **D'Amen M**, **Graham CH**, **Thuiller W**, **Zimmermann NE. 2010.** Within-taxon niche structure: niche conservatism, divergence and predicted effects of climate change. *Ecography* **33:** 990–1003.

Pérez-Ponce de León G, **Poulin R. 2016.** Taxonomic distribution of cryptic diversity among metazoans: not so homogeneous after all. *Biology Letters* **12:** 20160371–20160375.

Peterson AT. 2011. Ecological niche conservatism: a time-structured review of evidence. *Journal of Biogeography* **38:** 817–827.

Pisa S, **Werner O**, **Vanderpoorten A**, **Magdy M**, **Ros RM. 2013.** Elevational patterns of genetic variation in the cosmopolitan moss *Bryum argenteum* (Bryaceae). *American Journal of Botany* **100:** 2000–2008.

Poulin R, **Pérez-Ponce de León G. 2017.** Global analysis reveals that cryptic diversity is linked with habitat but not mode of life. *Journal of Evolutionary Biology* **30:** 641–649.

Puillandre N, **Brouillet S**, **Achaz G. 2019.** ASAP: assemble species by automatic partitioning. *Molecular Ecology Resources* **21:** 609–620.

Qiao H, **Escobar LE**, **Peterson AT. 2017.** Accessible areas in ecological niche comparisons of invasive species: recognized but still overlooked. *Scientific Reports* **7:** 1213.

Ramírez-Soriano A, **Ramos-Onsins SE**, **Rozas J**, **Calafell F**, **Navarro A. 2008.** Statistical power analysis of neutrality tests under demographic expansions, contractions and bottlenecks with recombination. *Genetics* **179:** 555–567.

R-Core-Team. **2019.** *R: a language and environment for statistical computing*. Vienna: R Project for Statistical Computing. Available at https://www.R-project.org/.

Shaw AJ. 1985. The relevance of ecology to species concepts in bryophytes. *Bryologist* **88:** 199–206.

Shaw AJ, **McDaniel SF**, **Werner O**, **Ros RM. 2002.** New frontiers in bryology and lichenology. Phylogeography and phylodemography. *Bryologist* **105:** 373–383.

Simmons MP, **Ochoterena H. 2000.** Gaps as characters in sequence-based phylogenetic analyses. *Systematic Biology* **49:** 369–381.

Simonsen KL, **Churchill GA**, **Aquadro CF. 1995.** Properties of statistical tests of neutrality for DNA polymorphism data. *Genetics* **141:** 413–429.

Singh P, **Ekrtová E**, **Holá E**, **Štechová T**, **Grill S**, **Hájek M. 2021.** Restoration of rare bryophytes in degraded rich fens: the effect of sod-and-moss removal. *Journal for Nature Conservation* **59:** 125928.

Smith AB, **Godsoe W**, **Rodríguez-Sánches F**, **Wang H-H**, **Warren D. 2019.** Niche estimation above and below the species level. *Trends in Ecology and Evolution* **34:** 260–273.

Snowden RED, **Wheeler BD. 1993.** Iron toxicity to fen plant species. *Journal of Ecology* **81:** 35–46.

Snowden RED, **Wheeler BD. 1995.** Chemical changes in selected wetland plant species with increasing Fe supply, with specific reference to root precipitates and Fe tolerance. *New Phytologist* **131:** 503–520.

Štechová T, **Kučera J**, **Šmilauer P. 2012.** Factors affecting population size and vitality of *Hamatocaulis vernicosus* (Mitt.) Hedenäs (Calliergonaceae, Musci). *Wetlands Ecology and Management* **20:** 329–339.

Struck TH, **Feder JL**, **Bendiksby M**, **Birkeland S**, **Cerca J**, **Gusarov VI**, **Kistenich S**, **Larsson K-H**, **Liow LH**, **Nowak MD**, **Stedje B**, **Bachmann L**, **Dimitrov D. 2018.** Finding evolutionary processes hidden in cryptic species. *Trends in Ecology and Evolution* **33:** 153–163.

Svenning J-C, **Skov F. 2007.** Could the tree diversity pattern in Europe be generated by postglacial dispersal limitation? *Ecology Letters* **10:** 453–460.

Taberlet P, **Fumagalli L**, **Wust-Saucy A-G**, **Cosson J-F. 1998.** Comparative phylogeography and postglacial colonization routes in Europe. *Molecular Ecology* **7:** 453–464.

Tajima F. 1989. Statistical method for testing the neutral mutation hypothesis by DNA polymorphism. *Genetics* **123:** 585–595.

Tollefsrud MM, **Kissling R**, **Gugerli F**, **Johnsen O**, **Skrøppa T**, **Cheddadi R**, **van der Knaap O**, **LataŁowa M**, **Terhürne-Berson R**, **Litt T**, **Geburek T**, **Brochmann C**, **Sperisen C. 2008.** Genetic consequences of glacial survival and postglacial colonization in Norway spruce: combined analysis of mitochondrial DNA and fossil pollen. *Molecular Ecology* **17:** 4134–4150.

Vanderpoorten A, **Durwael L. 1999.** Trophic response curves in lowland calcareous streams aquatic bryophytes. *Bryologist* **102:** 720–728.

Vanderpoorten A, **Shaw AJ. 2010.** The application of molecular data to the phylogenetic delimitation of species in bryophytes: a note of caution. *Phytotaxa* **9:** 229–237.

Vicherová E, **Hájek M**, **Hájek T. 2015.** Calcium intolerance of fen mosses: physiological evidence, effects of nutrient availability and successional drivers. *Perspectives in Plant Ecology, Evolution and Systematics* **17:** 347–359.

Wagner FS, **Wagner WH Jr. 1989.** Cryptic species, species delimitation, and taxonomic practice in homosporous ferns. *American Fern Journal* **79:** 46–54.

Warren DL, **Glor RE**, **Turelli M. 2008.** Environmental niche equivalency versus conservatism: quantitative approaches to niche evolution. *Evolution* **62:** 2868–2883.

Wheeler BD, **Al-Farraj MM**, **Cook RED. 1985.** Iron toxicity to plants in base-rich wetlands: comparative effects on the distribution and growth of *Epilobium hirsutum* L. and *Juncus subnodulosus* Schrank. *New Phytologist* **100:** 653–669.

APPENDIX 1

GenBank accession numbers for the studied *Hamatocaulis vernicosus* and outgroup specimens. Data format: **Sample No.[-sample classification as S or N (Cryptic species 1), or E or W (Cryptic species 2)]:** Locality; Collection date, *Collector [collector's no.];* Herbarium, [Herbarium no.]; GenBank accession numbers for ITS, *rpl16*, and *trnL-trnF*. [NA = not available].

***Hamatocaulis vernicosus* (Mitt.) Hedenäs. CRYPTIC SPECIES 1. M012-N:** Sweden. Småland, Källeryd; 1996, *L.Hedenäs & A.Kooijman*; S, B1070; DQ397055, DQ405051, DQ400063. **M013-N:** Sweden. Västergötland, Dala; 1996, *L.Hedenäs & A.Kooijman*; S, B1069; DQ397056, DQ405052, DQ400064. **M014-N:** Sweden. Västergötland, Valstad; 1996, *L.Hedenäs & A.Kooijman*; S, B1068; AY625994, DQ304456, AY626012. **M196-S:** Switzerland. Zürich, Wetzikon; 2002, *L.Hedenäs et al.*; S, B69400; DQ397085, DQ405079, DQ400092. **M197-S:** Switzerland. Zürich, Wetzikon; 2002, *L.Hedenäs et al.*; S, B69401; DQ397086, DQ405080, DQ400093. **M198-S:** Switzerland. Zürich, Mönchaltorf; 2002, *L.Hedenäs et al.*; S, B69402; DQ397087, DQ405081, DQ400094. **M199-S:** Switzerland. Zürich, Mönchaltorf; 2002, *L.Hedenäs et al.*; S, B69403; DQ397088, DQ405082, DQ400095. **M200-S:** Switzerland. Schwyz, Einsiedeln; 2002, *L.Hedenäs & E.Urmi*; S, B69404; DQ397089, DQ405083, DQ400096. **M384-N:** Sweden. Uppland, Jumkil; 1987, *L.Hedenäs*; S, B21439; EF172694, EF172729, EF172766. **M385-N:** Sweden. Småland, Höreda; 1999, *C.Jacobsson*; S, B24928; EF172695, EF172730, EF172767. **M386-N:** Sweden. Uppland, Edebo; 1997, *K.Hylander 2047*; S, B21370; EF172696, EF172731, EF172768. **M488:** United Kingdom. Cumbria, Great Ewe Fell; 1999, *D.T.Holyoak 99-1002*; S, B89325; NA, EF172735, EF172772. **M489-N:** United Kingdom. Wales, Gwynedd; 1999, *D.T.Holyoak 99-1968*; S, B89326; EF172700, EF172736, EF172773. **M490-N:** United Kingdom. Wales, Dyfed; 1999, *D.T.Holyoak 99-943*; S, B89327; EF172701, EF172737, EF172774. **M534-N:** Denmark. Viborg, Vinge Mølle; 2004, *L.Hedenäs*; S, B90388; EF172702, EF172738, EF172775. **M566:** Russia. Taimyr Peninsula, Nadaturku Lake; 1992, *E. Pospelova*; MW; EF172704, EF172740, EF172777. **M602:** Switzerland. Kt. Schwyz, Brunnen; 1990, *I.Bisang 90463*; S, 116576; NA, EF172741, EF172778. **M642-S:** Italy. Süd-Tirol, Eggental; 2005, *L.Hedenäs*; S, B103433; EF172705, EF172742, EF172779. **M676-S:** Austria. Carinthia, Klagenfurter Becken; 2005, *H.Köckinger*; S, B105473; EF172707, EF172744, EF172781. **M678-S:** Austria. Styria, S of Schladming; 2002, *R.Krisai*; S, B105475; EF172709, EF172746, EF172783. **M680-S:** Austria. Salzburg, Flachgau; 1999, *R.Krisai*; S, B105477;

EF172711, EF172748, EF172785. **M685-S:** Spain. Madrid, Sistema Central, Sierra de Guadarrama; 2004, *E.Fuertes et al.*; S, B107012; EF172715, EF172752, EF172789. **M707:** Peru. Cajamarca, N. Andes, Jalca; 2005, *D.J.Cooper 2825*; S, B108364; EF172716, EF172753, EF172790. **M834-N:** Netherlands. Overijssel, Weer.-Wieden NP, Kikkerl.; 2014, *L.Hedenäs et al.*; S, B211004; MZ417782, MZ447580, MZ447676. **M835-N:** Netherlands. Overijssel, Weer.-Wieden NP, Kiersche W.; 2014, *L.Hedenäs et al.*; S, B211009; MZ417783, MZ447581, MZ447677. **M836-N:** Netherlands. Overijssel, Weer.-Wieden NP, Veldweg; 2014, *L.Hedenäs et al.*; S, B211014; MZ417784, MZ447582, MZ447678. **M837-N:** Netherlands. Overijssel, Weer.-Wieden NP, Meppelerd.; 2014, *L.Hedenäs et al.*; S, B211016; MZ417785, MZ447583, MZ447679. **M838-N:** Netherlands. Gelderland, Epe, Korte Broek; 2014, *R.J.Bijlsma*; herb. Bijlsma, 15477.1; MZ417786, MZ447584, MZ447680. **M839-N:** Netherlands. Utrecht, Veenendaal, De Hel; 2009, *H.Runhaar*; herb. Siebel, 2009.830; MZ417787, MZ447585, MZ447681. **M840-N:** Netherlands. Staphorst, Oude Stroom NR; 2014, *M.van Tweel*; herb. van Tweel; MZ417788, MZ447586, MZ447682. **M952-N:** Sweden. Halland, Ledtorpet; 2016, *P.Darell*; S, B241054; MG952385, MG952289, MG952337. **M953-N:** Sweden. Småland, Jönköping, Dumme mosse; 2016, *P.Darell*; S, B241046; MG952386, MG952290, MG952338. **M954-N:** Sweden. Bohuslän, Säve, WSW Tomtebacken; 2010, *L.Appelgren*; S, B125425; MG952387, MG952291, MG952339. **M959-N:** Sweden. Västmanland, Sala, Kolarhagen; 2013, *L.Hedenäs*; S, B199749; MG952392, MG952296, MG952344. **M960-N:** Sweden. Västmanland, Sala, Kolarhagen; 2013, *L.Hedenäs*; S, B199755; MG952393, MG952297, MG952345. **M964-N:** Sweden. Uppland, Danmark, Norra Lunsen NR; 1998, *G.Aronsson*; S, B124245; MG952397, MG952301, MG952349. **M967-N:** Sweden. Dalarna, Grycksbo, Lilltansen; 2014, *U.Gunnarsson 1151*; S, B256788; MG952400, MG952304, MG952352. **M969-N:** Sweden. Dalarna, Sollerön, Norrviken; 2013, *U.Gunnarsson 1130*; S, B256793; MG952402, MG952306, MG952354. **M971-N:** Sweden. Skåne, Sankt Olof, SE of church; 2006, *J.Dahlberg*; S, B117507; MG952404, MG952308, MG952356. **M972-N:** Sweden. Småland, Jönköping, Rocksjön; 2009, *T.Fasth*; S, B172408; MG952405, MG952309, MG952357. **M973-N:** Sweden. Halland, Rollstorp; 2016, *P.Darell*; S, B241057; MG952406, MG952310, MG952358. **M974-N:** Sweden. Halland, Ö. Karup, Ledtorpet; 2008, *K Georgson*; S, B137494; MG952407, MG952311, MG952359. **M975-N:** Sweden. Västergötland, Otterstad, Kållandsö; 2008, *L.Hedenäs et al.*; S, B134501; MG952408, MG952312, MG952360. **M976-N:** Sweden. Närke, Örebro län, Bystadkvarnviken; 2016, *P.Darell*; S, B241043;

MG952409, MG952313, MG952361. **M977-N:** Sweden. Västmanland, Dragmossen; 2016, *P.Darell*; S, B241044; MG952410, MG952314, MG952362. **M979-N:** Sweden. Västmanland, Näset; 2016, *P.Darell*; S, B241056; MG952412, MG952316, MG952364. **M986-N:** Sweden. Östergötland, Blåvik; 2017, *M.Hagström*; S, B256797; MG952418, MG952323, MG952370. **M988:** Sweden. Östergötland, Torpa; 2017, *M.Hagström*; S, B256799; NA, NA, MG952372. **M989-N:** Sweden. Uppland, Värmdö, Koltorpsträsket; 1996, *N.Lönnell 26*; S, B258007; MG952420, MG952325, MG952373. **M990-N:** Sweden. Uppland, Västland, Barsjön; 2006, *N.Lönnell 2514*; S, B258010; MG952421, MG952326, MG952374. **M1530-S:** France. Ardèche, Cros-de-Géorand; 2018, *V.Hugonnot*; S, B297982; MZ417789, MZ447587, MZ447683. **M1531-S:** France. Puy de Dôme, Le Mont-Dore; 2017, *V.Hugonnot*; S, B297987; MZ417790, MZ447588, MZ447684. **M1532-S:** France. Bas Rhin, Belmont, Bar de la Reche; 2014, *V.Hugonnot*; S, B297988; MZ417791, MZ447589, MZ447685. **M1533-S:** France. Haute Loire, Saint-Paul-de-Tartas; 2012, *V.Hugonnot*; S, B297985; MZ417792, MZ447590, MZ447686. **M1534-S:** France. Savoie, Aillon-le-Jeune, Combe Levrier; 2014, *V.Hugonnot*; S, B297986; MZ417793, MZ447591, MZ447687. **M1537-S:** Serbia. SE-Serbia, Vlasina lake, Blato; 2010, *B.Papp 10/59/8*; BP, 184342; MZ417796, MZ447594, MZ447690. **M1538-N:** Ireland. Scragh bog near Lough Owel at Kilkbrackan; 2012, *B.Papp 12/110/4*; BP, 185753; MZ417797, MZ447595, MZ447691. **M1540-S:** Romania. Alcsík basin, Újtusnád, Varsavész; 2013, *B.Papp 13/72/7*; BP, 187892; MZ417799, MZ447597, MZ447693. **M1542-S:** Croatia. Plitvica NP, Plitvički Ljeskovac; 2013, *B.Papp 13/57/9*; BP, 188177; MZ417801, MZ447599, MZ447695. **M1543-S:** Serbia. Kopaonik Mts, Jankove bare; 2016, *J.Pantovic & B.Papp 16/52/4*; BP, 195809; MZ417802, MZ447600, MZ447696. **M1544-N:** Norway. Hordaland, Austrheim, Fonnes; 1972, *E.Fremstad*; BG, B6850; MZ417803, MZ447601, MZ447697. **M1545-N:** Norway. Hordaland, Bergen, Myravatn; 1978, *H.H.Blom*; BG, B6852; MZ417804, MZ447602, MZ447698. **M1559-N:** Finland. St., Karvia, Valtionmaa; 2002, *K.Syrjänen & T.Sallantus*; TUR, 101657; MZ417818, MZ447616, MZ447712. **M1561-N:** Finland. V., Kiikala, Komisuo; 2003, *K.Syrjänen & T.Sallantus*; TUR, 103211; MZ417820, MZ447618, MZ447714. **M1563-N:** Denmark. Vestjylland, Bredsgårde Sø; 2012, *K.Hassel & T.Høitomt*; TRH, 772680; MZ417822, MZ447620, MZ447716. **M1564-N:** Denmark. Vestjylland, Stubbergård Sø; 2012, *K.Hassel & T.Høitomt*; TRH, 772742; MZ417823, MZ447621, MZ447717. **M1567-S:** Germany. Baden-Württemberg, Hinterzarten; 2012, *K.Hassel*; TRH, 695264; MZ417826, MZ447624, MZ447720. **M1568-S:** Germany. Baden-Württemberg, Östl. Albvorland; 2009, *M.Sauer*; STU,

SMNS-B-BR-050748; MZ417827, MZ447625, MZ447721. **M1569-S:** Germany. Baden-Württemberg, Schwäb.-Fränk. Wald; 2011, *M.Sauer*; STU, SMNS-B-BR-050844; MZ417828, MZ447626, MZ447722. **M1570-S:** Germany. Baden-Württemberg, Oberschw., Osterried; 2011, *M.Sauer*; STU, SMNS-B-BR-050817; MZ417829, MZ447627, MZ447723. **M1573-S:** Austria. Vorarlberg, Allgäuer Alpen, Kleinwalsertal; 2011, *C.Schröck*; W, 0101434; MZ417832, MZ447630, MZ447726. **M1574-S:** Austria. Vorarlberg, Allgäuer Alpen, Tal der Bolgenach; 2010, *C.Schröck*; W, 0101376; MZ417833, MZ447631, MZ447727. **M1577-S:** Slovakia. Žilina Region, Svihrova NR; 2016, *K.Hassel*; TRH, 38133; MZ417836, MZ447634, MZ447730. **M1578:** Russia. Chukotka, Wrangel I.; 1985, *O.M.Afonina (Br. Ross.C.C.Ex. 89)*; STU, SMNS-B-BR-041047; MZ417837, MZ447635, MZ447731. **M1580-N:** Poland. Brzeźno Mazurskie, Dabrówno; 1997, *A.Łachacz 56/97*; KRAM, B-127254; MZ417839, MZ447637, MZ447733. **M1581-N:** Poland. Baltic Coast, Pojezierze Kaszubskie Lakel., L. Cheb; 1985, *B.P.Sagino*; KRAM, B-078960; MZ417840, MZ447638, MZ447734. **M1582-S:** Poland. Wyżyna Wieluńska, Trzebca; 1993, *B.Fojcik*; KRAM, B-110717; MZ417841, MZ447639, MZ447735. **M1583-N:** Poland. Pomorze Zachonie, Manowo; 2016, *A.Stebel*; KRAM, B-228346; MZ417842, MZ447640, MZ447736. **M1586-N:** Poland. N.R. Jeziorko koło Drozdowa; 2004, *E.Jabłońska*; KRAM, B-186327; MZ417845, MZ447643, MZ447739. **M1587-N:** Poland. Mazury, Puszcze Mazurskie, Zgon; 2007, *B.Hajek*; KRAM, B-228497; MZ417846, MZ447644, MZ447740. **M1588-S:** Poland. Karpaty Zachodnie, Beskid Makowsk; 1997, *A.Stebel 385/97*; KRAM, B-123324; MZ417847, MZ447645, MZ447741. **M1589-S:** Poland. Western Carpathians, Kotlina Orawsko-Nowotarska; 2016, *A.Stebel*; KRAM, B-228329; MZ417848, MZ447646, MZ447742. **M1590-N:** Poland. N.R. Sołtysek, Grom; 2004, *E.Jabłońska*; KRAM, B-186338; MZ417849, MZ447647, MZ447743. **M1592-N:** Poland. Pomorze Gdańskie, Ziemia Zaborska; 2007, *B.Hajek*; KRAM, B-228372; MZ417851, MZ447649, MZ447745. **M1689-S:** Spain. Cantabria, Valdeolea, Collado d Somah.; 2018, *P.Heras & M.Infante*; VIT, 39527 (77/18); MZ417853, MZ447651, MZ447747. **M1690-S:** Spain. Zamora, Galende, S. Martín d Castañ.; 2018, *P.Heras & M.Infante*; VIT, 39538 (88/18); MZ417854, MZ447652, MZ447748. **M1691:** Spain. Ávila, Hoyos del Espino, Sier. d Gredos; 2018, *P.Heras & M.Infante*; VIT, 29556 (106/18); NA, MZ447653, MZ447749. **M1692-S:** Spain. Burgos, Villamiel de la Sierra, Manantial d L. Burros; 1984, *P.Heras*; VIT, 5447 (1043/84); MZ417855, MZ447654, MZ447750. **M1693-S:** Spain. Soria, Vinuesa, Montes d Urbión; 2018, *P.Heras & M.Infante*; VIT, 39516 (66/18); MZ417856, MZ447655, MZ447751. **M1694-S:** France. Hautes Pyrénées, Arrens-Marsous; 2003, *M.Infante &*

P.Heras; VIT, 30487 (266/03); MZ417857, MZ447656, MZ447752. **M1696-S:** Switzerland. Kt. Sankt Gallen, Rapperwil-Jona; 2012, *N.Schnyder*; Z, 000137116; MZ417859, MZ447658, MZ447754. **M1697-S:** Switzerland. Kt. Sankt Gallen, Rapperwil-Jona; 2012, *N.Schnyder*; Z, 000137115; MZ417860, MZ447659, MZ447755. **JAN_8-S:** Czech Republic. Janovice, Pstruží potok; 2011, *Štechová 1160*; CBFS, 19354; MZ417862, MZ447661, MZ447757. **JAN_9-S:** Czech Republic. Rohozná, Nový rybník; 2011, *Štechová 1131*; CBFS, 19325; MZ417863, MZ447662, MZ447758. **JAN_16-S:** Czech Republic. Spolí, V Rájích; 2011, *Štechová 1133*; CBFS, 19327; MZ417864, MZ447663, MZ447759. **JAN_BD2b-S:** Czech Republic. Boží Dar, Božídarské rašeliniště; 2011, *Štechová 1139*; CBFS, 19333; MZ417866, MZ447665, MZ447761. **JAN_R42-S:** Czech Republic. Staré Ransko, Řeka; 2015, *Manukjanová s.n.*; CBFS, 22835; MZ417867, MZ447666, MZ447762. **JAN_ru3:** Russia. Buryatia, Usť-Barguzin, Svyatoy Nos; 2013, *Koutecký*; CBFS, 22839; MZ417869, MZ447668, MZ447764. **JAN_V10b-S:** Czech Republic. Hrubá Skála, Vidlák; 2013, *Manukjanová s.n.*; CBFS, 22836; MZ417870, MZ447669, MZ447765. **JAN_Zh6-S:** Czech Republic. Čachrov, Zhůří; 2013, *Manukjanová s.n.*; CBFS, 22834; MZ417872, MZ447671, MZ447767. **CRYPTIC SPECIES 2. M015-W:** Sweden. Västergötland, Sandhem; 1992, *L.Hedenäs*; S, 21467; DQ397057, DQ405053, DQ400065. **M016-W:** Sweden. Södermanland, Österåker; 1993, *L.Hedenäs*; S, B21425; DQ397058, DQ405054, DQ400066. **M017-E:** Sweden. Uppland, Malsta; 1996, *L.Hedenäs & K.Hylander*; S, B1073; DQ397059, DQ405055, DQ400067. **M018-E:** Sweden. Uppland, Lohärad; 1996, *L.Hedenäs & K.Hylander*; S, B1071; DQ397060, DQ405056, DQ400068. **M019-E:** Sweden. Uppland, Edsbro; 1996, *L.Hedenäs & K.Hylander*; S, B1072; DQ397061, DQ405057, DQ400069. **M020-E:** Sweden. Uppland, Älvkarleby; 1992, *L.Hedenäs*; S, B21454; DQ397062, DQ405058, DQ400070. **M021-W:** Sweden. Jämtland, Hammerdal; 1997, *L.Hedenäs & A.Kooijman*; S, B1459; DQ397063, DQ405059, DQ400071. **M022-W:** Sweden. Jämtland, Lit; 1997, *L.Hedenäs & A.Kooijman*; S, B1477; DQ397064, DQ405060, DQ400072. **M023-E:** Sweden. Åsele lappmark, Vilhelmina, Blomsterm.; 1991, *L.Hedenäs & A.Kooijman*; S, B21478; DQ397065, DQ405061, DQ400073. **M024-E:** Sweden. Åsele lappmark, Vilhelmina, Främmerm.; 1991, *L.Hedenäs & A.Kooijman*; S, B21481; DQ397066, DQ405062, DQ400074. **M025-E:** Sweden. Lule lappmark, Jokkmokk, Sasnekape; 1991, *L.Hedenäs & A.Kooijman*; S, B21395; DQ397067, DQ405063, DQ400075. **M026:** U.S.A. Minnesota, Itasca Co., Wirt Area; 1999, *L.Hedenäs & J.A.Janssens*; S, B16964; DQ397068, DQ405064, DQ400076. **M027:** U.S.A. Minnesota,

Koochiching Co., Waskish Area; 1999, *L.Hedenäs & J.A.Janssens*; S, B16965; DQ397069, DQ405065, DQ400077. **M028:** U.S.A. Minnesota, Beltrami Co., Kelliher Area; 1999, *L.Hedenäs & J.A.Janssens*; S, B16966; DQ397070, DQ405066, DQ400078. **M029:** U.S.A. Minnesota, Clearwater Co., Itasca Area; 1999, *L.Hedenäs & J.A.Janssens*; S, B16967; DQ397071, DQ405067, DQ400079. **M030:** U.S.A. Minnesota, Clearwater Co., Itasca Area; 1999, *L.Hedenäs & J.A.Janssens*; S, B16968; DQ397072, DQ405068, DQ400080. **M031:** U.S.A. Minnesota, Clearwater Co., Itasca Area; 1999, *L.Hedenäs & J.A.Janssens*; S, B16969; DQ397073, DQ405069, DQ400081. **M032:** U.S.A. Minnesota, Becker Co., Itasca Area; 1999, *L.Hedenäs & J.A.Janssens*; S, B16970; DQ397074, DQ405070, DQ400082. **M033:** U.S.A. Minnesota, Cass Co., Bena Area; 1999, *L.Hedenäs & J.A.Janssens*; S, B16971; DQ397075, DQ405071, DQ400083. **M034:** U.S.A. Minnesota, Cass Co., Deer River Area; 1999, *L.Hedenäs & J.A.Janssens*; S, B16972; DQ397076, DQ405072, DQ400084. **M069-W:** Sweden. Västergötland, N. Kyrketorp; 1992, *L.Hedenäs*; S, B21465; DQ397077, DQ405073, DQ400085. **M155-W:** Sweden. Jämtland, Mörsil, Djupmyren; 2001, *L.Hedenäs*; S, B61853; DQ397079, DQ405074, DQ400086. **M158-W:** Sweden. Jämtland, Mörsil, Strömdrolet; 2001, *L.Hedenäs*; S, B61856; DQ397080, DQ405075, DQ400087. **M159-W:** Sweden. Jämtland, Mörsil, Strömdrolet; 2001, *L.Hedenäs*; S, B61857; DQ397081, DQ405076, DQ400088. **M165-W:** Sweden. Jämtland, Mattmar, Movallsflon; 2001, *L.Hedenäs*; S, B61863; DQ397082, DQ405077, DQ400089. **M168-W:** Sweden. Jämtland, Mörsil, Edstjärnen; 2001, *L.Hedenäs*; S, B61866; DQ397083, DQ304457, DQ400090. **M195-W:** Switzerland. Sankt Gallen, Ebnat-Kappel; 2002, *L.Hedenäs*; S, B69398; DQ397084, DQ405078, DQ400091. **M214-E:** Sweden. Uppland, Hökhuvud; 2002, *L.Hedenäs*; S, B70224; DQ397078, DQ405084, DQ400097. **M273-E:** Sweden. Torne lappmark, Jukkasjärvi, Anterusvuoma; 2002, *L.Hedenäs*; S, B72998; DQ397090, DQ405085, DQ400098. **M274-E:** Sweden. Torne lappmark, Jukkasjärvi, Anterusvuoma; 2002, *L.Hedenäs*; S, B72999; DQ397091, DQ405086, DQ400099. **M275-E:** Sweden. Torne lappmark, Jukkasjärvi, Lake Syöttöjärvi; 2002, *L.Hedenäs*; S, B73000; DQ397092, DQ405087, DQ400100. **M372-W:** Sweden. Dalarna, Älvdalen; 1995, *L.Bratt*; S, B21358; EF172682, EF172717, EF172754. **M373-E:** Sweden. Hälsingland, Rogsta, Änga; 1993, *J.Abenius*; S, B21380; EF172683, EF172718, EF172755. **M374-W:** Sweden. Härjedalen, Sveg, Lakes Sjuartjärnarna; 1989, *L.Hedenäs*; S, B21375; EF172684, EF172719, EF172756. **M375-E:** Sweden. Lule lappmark, Gällivare, Kievavuoma; 1999, *Wetland Survey Nb*; S, B110520; EF172685, EF172720, EF172757. **M376-E:** Sweden. Lule lappmark,

Gällivare, Sjaunja-ape; 2000, *Wetland Survey Nb*; S, B110526; EF172686, EF172721, EF172758. **M377-E:** Sweden. Norrbotten, Pajala, Kursuvuoma; 2002, *Wetland Survey Nb*; S, B110549; EF172687, EF172722, EF172759. **M378-E:** Sweden. Norrbotten, Nederkalix, Mjöträsket; 1998, *Wetland Survey Nb*; S, B110510; EF172688, EF172723, EF172760. **M379-E:** Sweden. Torne lappmark, Karesuando, Rajavuoma; 2003, *S.Westerberg*; S, B110560; EF172689, EF172724, EF172761. **M380-W:** Sweden. Jämtland, Aspås, Källmyran; 2001, *K.Hylander 2847*; S, B64085; EF172690, EF172725, EF172762. **M381-W:** Sweden. Jämtland, Gåxsjö, Kälaslåtten; 1989, *L.Hedenäs*; S, B21384; EF172691, EF172726, EF172763. **M382-E:** Sweden. Åsele lappmark, Vilhelmina, Stormyran; 1987, *L.Hedenäs*; S, B21577; EF172692, EF172727, EF172764. **M383-W:** Sweden. Närke, Lerbäck, Sörsjön; 1992, *N.Hakelier*; S, B21502; EF172693, EF172728, EF172765. **M387-E:** Sweden. Upland, Fasterna; 1997, *K.Hylander 1998*; S, B21426; EF172697, EF172732, EF172769. **M388-E:** Sweden. Uppland, Häverö; 1996, *K.Hylander 1928*; S, B21438; EF172698, EF172733, EF172770. **M390-W:** Poland. W. Pomerania, Kartuzy Lake District; 1989, *H.Bednarek-Ochyra & R.Ochyra (Musci Pol.Ex. 1068)*; S, B22081; EF172699, EF172734, EF172771. **M535-W:** Denmark. Viborg, Lake Kvorning Møllesø; 2004, *L.Hedenäs*; S, B90391; EF172703, EF172739, EF172776. **M643-W:** Italy. Süd-Tirol, Wolkenstein, Juac; 2005, *L.Hedenäs*; S, B103434; EF172706, EF172743, EF172780. **M677-W:** Austria. Carinthia, Klagenfurter Becken, NE Villach; 2005, *H.Köckinger*; S, B105474; EF172708, EF172745, EF172782. **M679-W:** Austria. Upper Austria, Gosau, Zwieselberg; 1999, *R.Krisai*; S, B105476; EF172710, EF172747, EF172784. **M681-W:** Austria. Salzburg, Pongau, Dientener Sattel; 2001, *R.Krisai*; S, B105478; EF172712, EF172749, EF172786. **M682-W:** Austria. Upper Austria, St. Wolfgang, Moosalm Moor; 2001, *R.Krisai*; S, B105479; EF172713, EF172750, EF172787. **M683-W:** Sweden. Västmanland, Viker, Bromossen; 2005, *L.Hedenäs*; S, B104644; EF172714, EF172751, EF172788. **M955-W:** Sweden. Västergötland, Slöta, Sjöängen; 2016, *L.Appelgren*; S, B125424; MG952388, MG952292, MG952340. **M956-W:** Sweden. Västergötland, Valstad, Gorsorna; 2006, *L.Appelgren*; S, B125423; MG952389, MG952293, MG952341. **M957-W:** Sweden. Värmland, Nordmark, Nordmarksmyrarna; 2006, *N.Lönnell 3017*; S, B242751; MG952390, MG952294, MG952342. **M958-W:** Sweden. Västmanland, Venakärret; 2014, *J.Hansson*; S, B204131; MG952391, MG952295, MG952343. **M961-W:** Sweden. Närke, Lerbäck, Sörsjön; 1999, *Å.Lindström*; S, B17014; MG952394, MG952298, MG952346. **M962-E:** Sweden. Uppland, Bladåker; 1993, *T.Hallingbäck 46320*; S, B202513; MG952395, MG952299, MG952347. **M963-E:** Sweden. Uppland,

Västland; 2006, *N.Lönnell 2514*; S, B117018; MG952396, MG952300, MG952348. **M965-W:** Sweden. Dalarna, Gagnef, Trolldalen; 1993, *L.Hedenäs*; S, B21350; MG952398, MG952302, MG952350. **M966-E:** Sweden. Gästrikland, Gävleborg, Gustavmurarna; 2016, *P.Darell*; S, B241051; MG952399, MG952303, MG952351. **M968-W:** Sweden. Dalarna, Ore, Moränget; 2010, *U.Gunnarsson 1019*; S, B256792; MG952401, MG952305, MG952353. **M970-W:** Sweden. Dalarna, Äppelbo, Bosarflotten; 2012, *U.Gunnarsson 1123*; S, B256794; MG952403, MG952307, MG952355. **M978-W:** Sweden. Västmanland, Gransjön; 2016, *P.Darell*; S, B241050; MG952411, MG952315, MG952363. **M980-E:** Sweden. Uppland, Förrådet; 2016, *P.Darell*; S, B241049; MG952413, MG952317, MG952365. **M981-E:** Sweden. Uppland, Tisselhararna; 2016, *P.Darell*; S, B241059; MG952414, MG952318, MG952366. **M982-W:** Sweden. Dalarna, Holsmyran; 2016, *P.Darell*; S, B241052; MG952415, MG952319, MG952367. **M983:** Sweden. Dalarna, Malung, Vimyren; 1944, *H.Sjörs 35*; S, B21353; NA, MG952320, NA. **M984-W:** Sweden. Östergötland, Malexander, Axsjön; 2017, *M.Hagström*; S, B256795; MG952416, MG952321, MG952368. **M985-W:** Sweden. Östergötland, Blåvik, Funkenkärret; 2017, *M.Hagström*; S, B256796; MG952417, MG952322, MG952369. **M987-W:** Sweden. Östergötland, Asby, Skogsgölen; 2017, *M.Hagström*; S, B256798; MG952419, MG952324, MG952371. **M991-E:** Sweden. Ångermanland, Helgum, Prästflon; 2006, *N.Lönnell 4434*; S, B258016; MG952422, MG952327, MG952375. **M1022-E:** Sweden. Gästrikland, Gävle, Matyxsjön; 2017, *T.Troschke*; S, B259491; MG952423, MG952328, MG952376. **M1023-E:** Sweden. Gästrikland, Gävle, Bläcktärnsjön; 2017, *T.Troschke*; S, B259492; MG952424, MG952329, MG952377. **M1024-W:** Sweden. Värmland, Norra Finnskoga, Bringsåsen; 2012, *N.Lönnell 3603*; S, B259697; MG952425, MG952330, MG952378. **M1025-E:** Sweden. Jämtland, Ragunda, Grånmyran; 2001, *K.Hylander 2848*; S, B64084; MG952426, MG952331, MG952379. **M1026-W:** Sweden. Uppland, Huddunge, Huddunge Stormosse; 2008, *T.Pettersson*; S, B260442; MG952427, MG952332, MG952380. **M1027-W:** Sweden. Västmanland, Ramnäs, Färmensbo; 2008, *T.Pettersson*; S, B260444; MG952428, MG952333, MG952381. **M1028-W:** Sweden. Västmanland, Viker, Näsmarkerna; 2007, *T.Pettersson*; S, B260446; MG952429, MG952334, MG952382. **M1029-W:** Sweden. Västmanland, Västanfors, Morbymossen; 2003, *T.Pettersson*; S, B260447; MG952430, MG952335, MG952383. **M1030-W:** Sweden. Uppland, Norrby, Klasbo; 2004, *T.Pettersson*; S, B260448; MG952431, MG952336, MG952384. **M1535-W:** Romania. Muntii Gilaului, Belis-Dealu Negru; 2006, *T.Pócs & K.Buczkó 06083/B*; BP, 177092; MZ417794, MZ447592, MZ447688.

M1536-W: Montenegro. Crna Gora, Durmitor Mts, Žabljak; 2004, *B.Papp 04 / 93 / 9*; BP, 178955; MZ417795, MZ447593, MZ447689. **M1539-W:** Romania. Alcsík basin, Csíkszentsimon, Felső Honcsok; 2013, *B.Papp 13 / 65 / 11*; BP, 187849; MZ417798, MZ447596, MZ447692. **M1541-W:** Serbia. Southern-Serbia, Pešter plateau, Kneževac; 2012, *B.Papp 12 / 51 / 10*; BP, 186668; MZ417800, MZ447598, MZ447694. **M1546-W:** Norway. Oppland, Nordre Land, Gygertjernet; 2011, *T.Høitomt 11254M*; TRH, 771355; MZ417805, MZ447603, MZ447699. **M1547-W:** Norway. Oppland, Svarttjørn; 2011, *T.Høitomt 11076M*; TRH, 674816; MZ417806, MZ447604, MZ447700. **M1548-E:** Finland. Pohjois-Savo, Joroinen, Tervaruukinsalo; 2013, *S.Huttunen*; TUR, 118053; MZ417807, MZ447605, MZ447701. **M1549-E:** Finland. EH. Kalvola, Isosuo, Hietamäen talosta; 2004, *T.Hayhä*; TUR, 104411; MZ417808, MZ447606, MZ447702. **M1550-E:** Finland. (ESA 2b), Pieksämäki, Jäppilä, Maijootsuo; 2013, *T.Marsh & K.Pihlaja*; TUR, 118598; MZ417809, MZ447607, MZ447703. **M1551-E:** Finland. V (UUS 1b), Karjalhja, Tulijärven suot; 2002, *T.Sallantus 7*; TUR, 101684; MZ417810, MZ447608, MZ447704. **M1552-E:** Finland. Oulun Pohjanmaa, Oulu, Kiiminki; 2018, *K.Pihlaja*; TUR, 124236; MZ417811, MZ447609, MZ447705. **M1553-E:** Finland. Kainuu, Paltamo, Kontiomäki; 1997, *K.Syrjänen*; TUR, 118234; MZ417812, MZ447610, MZ447706. **M1554-E:** Finland. Kn., Puolanka, Alajakso, Kapustajoen poh.; 1997, *K.Syrjänen & T.Ryttäri*; TUR, 104345; MZ417813, MZ447611, MZ447707. **M1555-E:** Finland. Oulun Pohjanmaa, Ii, Kuivaniemi, Luujoki; 2018, *K.Pihlaja*; TUR, 124214; MZ417814, MZ447612, MZ447708. **M1556-E:** Finland. Oulun Pohjanmaa, Pudasjärvi, Puhos, Lianlampi; 2018, *K.Pihlaja*; TUR, 124222; MZ417815, MZ447613, MZ447709. **M1557-E:** Finland. Ahvenanmaa, Hammarland, Westmyra; 2010, *T.Häyhä*; TUR, 114235; MZ417816, MZ447614, MZ447710. **M1558-E:** Finland. SoL, Pelkoseniemi, Alaperä, Sudenvaaranaapa; 2002, *K.Syrjänen*; TUR, 101986; MZ417817, MZ447615, MZ447711. **M1560-E:** Finland. KiL, Kolari, Sieppijärvi, Kuurusenvuoma; 2002, *K.Syrjänen & P.Paalamo*; TUR, 101961; MZ417819, MZ447617, MZ447713. **M1562-E:** Russia. Karelia, Karelia Onegensis, Medvežjagorski raion; 2013, *K.Syrjänen*; TUR, 118247; MZ417821, MZ447619, MZ447715. **M1565-E:** Estonia. Lääne-Virumaa, Äntu lakes; 2012, *M.Olsen Kyrkjeeide & K.I.Flatberg*; TRH, 120289; MZ417824, MZ447622, MZ447718. **M1566-E:** Estonia. Valgamaa, Päästjärve mire; 2012, *M.Olsen Kyrkjeeide & K.I.Flatberg*; TRH, 120259; MZ417825, MZ447623, MZ447719. **M1571-W:** Germany. Baden-Württemberg, Wolpertswende; 2014, *M.Sauer*; STU, SMNS-B-BR-056080; MZ417830, MZ447628, MZ447724. **M1572-W:** Germany. Bayern, Oberallgäu, Kematsriedmoos; 2004, *M.Preussing*; STU, SMNS-B-BR-001842; MZ417831, MZ447629, MZ447725. **M1575-W:** Austria. Vorarlberg, Bregenzerwald, Schönenbachvorsäss; 2010, *C.Schröck*; W, 0101433; MZ417834, MZ447632, MZ447728. **M1576-W:** Austria. Vorarlberg, Bregenzerwald, Bezau; 2010, *C.Schröck*; W, 0101368; MZ417835, MZ447633, MZ447729. **M1579-E:** Poland. Pojezierze Litewskie, Pojezierze Wschodniosuw.; 1994, *A.Łachacz*; KRAM, B-110130; MZ417838, MZ447636, MZ447732. **M1584-E:** Poland. Nizina Północnopodlaska, Kotlina, Biebrzańska; 2016, *A.Stebel*; KRAM, B-231271; MZ417843, MZ447641, MZ447737. **M1585-E:** Poland. Augustów Forest, Borsuki Peatland; 2004, *E.Jabłońska*; KRAM, B-186343; MZ417844, MZ447642, MZ447738. **M1591-W:** Poland. W Carpathias, Beskid Maly; 1996, *A.M.Stebel & A.Stebel 381 / 96*; KRAM, B-120992; MZ417850, MZ447648, MZ447744. **M1650-W:** Austria. Rodarm; 2020, *E.Mikulášková & T.Peterka*; BRNU, 648289; MZ417852, MZ447650, MZ447746. **M1695-W:** Switzerland. Kt. Bern, Lauterbrunnen, Untersteinb.; 1998, *Wirkungsk. Moorbiotope*; Z, 000137112; MZ417858, MZ447657, MZ447753. **M1698-W:** Switzerland. Kt. Bern, Gemeinde Lauenen, Fang; 2019, *Projekt Rote Liste 2020*; Z, 000137114; MZ417861, MZ447660, MZ447756. **JAN_BD1b-W:** Czech Republic. Boží Dar, Božídarské rašeliniště; 2011, *Štechová 1138*; CBFS, 19332; MZ417865, MZ447664, MZ447760. **JAN_R53-W:** Czech Republic. Staré Ransko, Řeka; 2015, *Manukjanová s.n.*; CBFS, 22838; MZ417868, MZ447667, MZ447763. **JAN_Zh3j-W:** Czech Republic. Čachrov, Zhůří; 2015, *Manukjanová s.n.*; CBFS, 22837; MZ417871, MZ447670, MZ447766. **OUTGROUP SPECIES:** *Hamatocaulis lapponicus* **(Norrl.) Hedenäs. M356:** U.S.A. Alaska, Kuskokwim/ Yukon Delta, Bethel; 2001, *K.Thingsgaard & K.I.Flatberg 01-438*; S, B61299; AY625989, DQ405088, AY626008. *Scorpidium cossonii* **(Schimp.) Hedenäs. M119:** Sweden. Jämtland, Åre, Fröån; 2001, *L.Hedenäs*; S, B61807; AY625996, DQ304458, AY626013. *Scorpidium revolvens* **(Sw. ex Anonymo) Rubers. M282:** Sweden. Torne lappmark, Jukkasjärvi, Vastakielisenvaara; 2002, *L.Hedenäs*; S, B73007; AY625998, MZ447579, AY626019. *Scorpidium scorpioides* **(Hedw.) Limpr. M139:** Sweden. Jämtland, Undersåker, Sönner-Välaflon; 2001, *L.Hedenäs*; S, B61836; AY625995, DQ410038, AY626014.
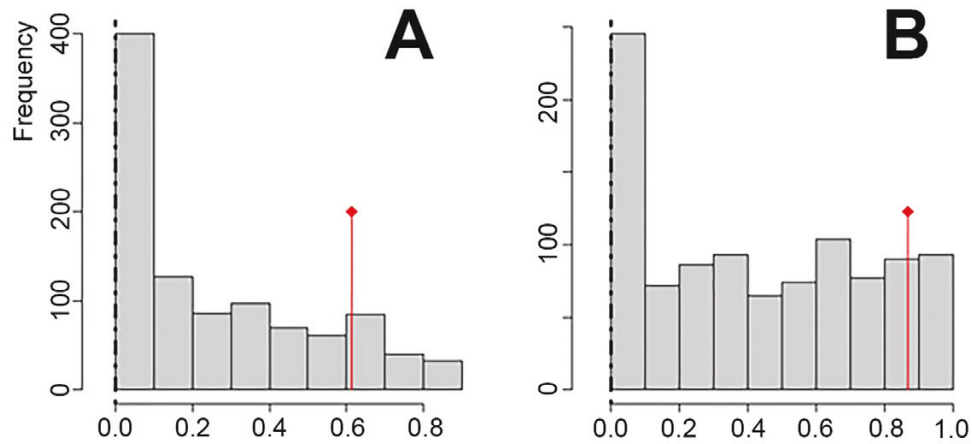
APPENDIX 2

Climatic variables at 1-km resolution used for the climatic niche preferences. The corresponding names from CHELSA and how they were generated and their units are present in the second column.

Climatic variables	Variables from CHELSA (unit)
Annual mean temperature	Bio 1 (°C)
Annual range of temperature	Bio 7 (°C)
Mean temperature of the wettest quarter	Bio 8 (°C)
Annual precipitation	Bio 12 (mm)
Precipitation seasonality	Bio 15 (kg m^{-2})
Precipitation of the warmest quarter	Bio 18 (mm)
Annual mean relative humidity	Average of the monthly relative humidity [rh] (%)
Annual mean solar radiation	Average of the monthly total solar radiation [srad] (kJ m^{-2})
Annual range of solar radiation	Difference between the maximum and the minimum values generated from monthly total solar radiation [srad] (kJ m^{-2})
Annual mean potential evapotranspiration	Average of monthly potential evapotranspiration [pet] (kg m^{-2})
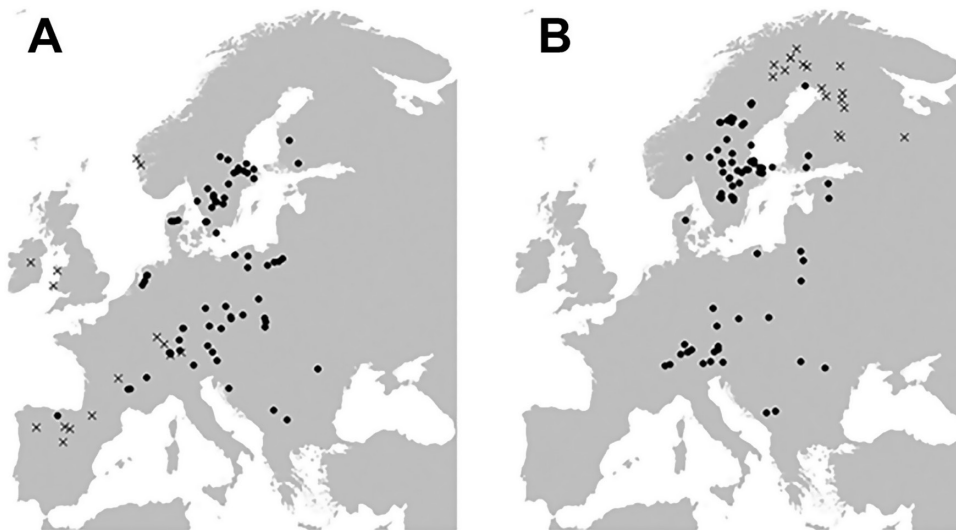
Appendix 3. Results of the MESS analyses for CRS1 (A) and CRS2 (B). Dots represent the occurrences used for niche overlap computations and niche comparisons, whereas crosses correspond to the occurrences that were removed from the analyses..

Appendix 4. Null distributions of niche overlap computed with the Schoener's *D* (A) and Hellinger's *I* (B) metrics, resulting from the niche similarity test. Vertical lines in red (colour only online) with diamond on top represents the observed niche overlap between the two cryptic species, whereas the dark grey dotted lines represent the 95% confidence interval limits of null distributions.